Expert Opinion on Drug Delivery

ISSN: 1742-5247 (Print) 1744-7593 (Online) Journal homepage: http://www.tandfonline.com/loi/iedd20

Superparamagnetic iron oxide nanoparticles for delivery of therapeutic agents: opportunities and challenges

Sophie Laurent, Amir Ata Saei, Shahed Behzadi, Arash Panahifar & Morteza Mahmoudi

To cite this article: Sophie Laurent, Amir Ata Saei, Shahed Behzadi, Arash Panahifar & Morteza Mahmoudi (2014) Superparamagnetic iron oxide nanoparticles for delivery of therapeutic agents: opportunities and challenges, Expert Opinion on Drug Delivery, 11:9, 1449-1470, DOI: 10.1517/17425247.2014.924501

To link to this article: https://doi.org/10.1517/17425247.2014.924501

Published online: 29 May 2014.

EXPERT OPINION

Superparamagnetic iron oxide nanoparticles for delivery of therapeutic agents: opportunities and challenges

Sophie Laurent[†], Amir Ata Saei, Shahed Behzadi, Arash Panahifar & Morteza Mahmoudi

[†]*University of Mons, Avenue Maistriau, NMR and Molecular Imaging Laboratory, Department of General, Organic, and Biomedical Chemistry, Mons, Belgium*

Introduction: Bearing in mind that many promising drug candidates have the problem of reaching their target site, the concept of advanced drug delivery can play a significant complementary role in shaping modern medicine. Among other nanoscale drug carriers, superparamagnetic iron oxide nanoparticles (SPIONs) have shown great potential in nanomedicine. The intrinsic properties of SPIONs, such as inherent magnetism, broad safety margin and the availability of methods for fabrication and surface engineering, pave the way for diverse biomedical applications. SPIONs can achieve the highest drug targeting efficiency among carriers, since an external magnetic field locally applied to the target organ enhances the accumulation of magnetic nanoparticles in the drug site of action. Moreover, theranostic multifunctional SPIONs make simultaneous delivery and imaging possible. In spite of these favorable qualities, there are some toxicological concerns, such as oxidative stress, unpredictable cellular responses and induction of signaling pathways, alteration in gene expression profiles and potential disturbance in iron homeostasis, that need to be carefully considered. Besides, the protein corona at the surface of the SPIONs may induce few shortcomings such as reduction of SPIONs targeting efficacy.

Areas covered: In this review, we will present recent developments of SPIONs as theranostic agents. The article will further address some barriers on drug delivery using SPIONs.

Expert opinion: One of the major success determinants in targeted *in vivo* drug delivery using SPIONs is the adequacy of magnetic gradient. This can be partially achieved by using superconducting magnets, local implantation of magnets and application of magnetic stents. Other issues that must be considered include the pharmacokinetics and *in vivo* fate of SPIONs, their biodegradability, biocompatibility, potential side effects and the crucial impact of protein corona on either drug release profile or mistargeting. Surface modification of SPIONs can open up the possibility of drug delivery to intracellular organelles, drug delivery across the blood–brain barrier, modifying metabolic diseases and a variety of other multimodal and/or theranostic applications.

Keywords: biomedical, biomedicine, coating, controlled release, functionalization, nanocarrier, surface targeting, toxicity

Expert Opin. Drug Deliv. (2014) ***11****(9):1449-1470*

informa
healthcare

10.1517/17425247.2014.924501 ISSN 1742-5247, e-ISSN 1744-7593

Article highlights.

- Superparamagnetic iron oxide nanoparticles (SPIONs) can be incorporated into various homing nanostructures to produce biodevices, including drug delivery systems and MRI contrast agents.
- Owing to their intrinsic superparamagnetism, SPION-harboring formulations can be guided by extrinsic magnetic fields to a desired *in vivo* location.
- The biocompatibility and stability of SPIONs can be enhanced by the type of coating.
- SPIONs can be functionalized with targeting moieties to enhance the accumulation of therapeutics in their site of action.
- The versatility of SPIONs allows the production of theranostic, multimodal and multifunctional devices that can be used for simultaneous drug delivery and imaging, biomolecular tracking and cell labeling.
- Protein corona can change the drug release profile and relaxivity of SPIONs.
- Protein corona can cover the targeting moieties at the surface of the SPIONs and decrease their targeting yield.

This box summarizes key points contained in the article.

1. Introduction

Theranostic nanoscale systems combine the modalities of therapy and diagnosis in a smart device, allowing for drug delivery and real-time diagnostic imaging at the same time [1]. Among numerous drug delivery systems (DDSs), magnetic nanoparticles (NPs) such as superparamagnetic iron oxide nanoparticles (SPIONs), a subclass of theranostic systems, have gained significant attention in the past decades [2]. Drug/SPION-loaded NPs or drug-bound SPIONs can be used for simultaneous magnetic resonance/optical/ positron-emission tomography (PET)/single-photon-emission computed tomography (SPECT)/fluorescence imaging, drug delivery and real-time monitoring of therapeutic response in theranostic systems and have been recently reviewed by Yen *et al.* [3]. The theranostics capability of the SPIONs along with their higher biocompatibility compared to the other DDSs, makes them more attractive candidates for drug delivery applications. Although biodegradability and elimination are major issues with other DDSs, SPIONs are usually metabolized and excreted from the body through the endogenous iron metabolic pathway [4,5]. Other DDSs such as polymeric NPs, liposomal systems and micelles suffer from limited chemical and mechanical stability, polydispersity, unpredictable pharmacological properties and inadequate control over the drug release rate [6].

SPIONs are NPs with a synthetic γ-Fe_2O_3 (maghemite), Fe_3O_4 (magnetite) or α-Fe_2O_3 (hematite) core. Mixed transition metal oxides (copper, cobalt, nickel and manganese) with iron oxide also exhibit superparamagnetic properties and are members of the SPIONs family.

SPIONs exhibit a range of favorable properties, including intrinsic magnetism for MRI, safety and availability of biocompatible coatings and surface functional moieties. These virtues have opened up a large range of possible biomedical applications of SPIONs in drug delivery [7], *in vivo* medical imaging [8], biosensing [9], regenerative medicine [10] and hyperthermia [11].

SPION-based DDSs are commonly composed of magnetite and maghemite NPs with an organic or inorganic coating. These magnetic drug-bearing nanostructures rely on external magnetic field guidance to reach their target tissue. Magnetic vehicles, including magnetic capsules, magnetoliposomes or magnetodendrimers reduce the clearance of drugs and increase their blood circulation time. They also increase drug internalization efficiency within target cells and minimize nonspecific cellular interactions, thus reducing the total required dose and associated side effects. Owing to their unique superparamagnetic characteristics (which are usually observed for NPs with a diameter of 6 – 25 nm), SPIONs become magnetized up to their saturation magnetization using an external magnetic field and gain high magnetic susceptibility. On removal of the magnetic field, no magnetic interaction is observed. In this way, SPIONs acquire the capability to drag the encapsulated or attached drug to the target site in the body under the externally applied magnetic field and are inactivated on the removal of the magnetic field. However, further research is required to gain a thorough knowledge of the toxicity of SPIONs and their interactions with biomolecules, organelles, cells and biological systems.

In this article, we will review the recent advances in the use of SPIONs for drug delivery and imaging applications. In addition, the challenges in the field together with the future directions would be discussed.

2. Preparation and surface modification of SPIONs with functional moieties

Both top-down mechanical attrition and bottom-up approaches have been developed for SPIONs synthesis. Broadly classified, SPIONs synthesis falls into physical, biological and chemical routes. Physical methods include gas phase deposition, electron beam lithography, pulsed laser ablation, laser-induced pyrolysis, powder ball milling and aerosol production. Further, SPIONs might be produced through the biological activity of fungi, bacteria and even proteins such as ferritin and Mms6 [2]. Chemical techniques provide a better consistency of size and composition; they include standard iron chloride coprecipitation, thermal decomposition, microemulsion, hydrothermal synthesis and sonochemical methods, which are explained below. Details on the diverse preparation approaches can be found in our previous comprehensive review [2].

Despite the fact that naked SPIONs are stable in high- and low-pH suspensions and not in the neutral pH, they must be coated for *in vivo* applications. A surface coating may be exploited to: i) increase the stability and protect NPs against

agglomeration; ii) protect the magnetic core against oxidation; iii) provide a reactive surface to accommodate drug molecules or targeting ligands; iv) add to the biocompatibility of DDSs by limiting nonspecific interactions; v) protect NPs against reticuloendothelial system (RES) uptake and elimination, thus increasing the blood circulation time; and vi) enhance the NP's internalization efficiency. Coatings largely influence the functionality and biological fate of DDSs. For example, coating NPs with hydrophilic polymers, including PEG, poloxamers, polysorbate 20 and 80, tocopheryl PEG succinate and dextran, can inhibit the formation of a protein layer at the particle's surface by providing a hydrophilic cloud and neutral chains [12]. Although PEGylation improves the pharmacokinetic profile of DDSs and enhances the accumulation of nanoscale DDS in tumor [13], coating with polysorbate has been shown to improve the blood–brain barrier (BBB) transport of NPs [14].

In the literature, the main SPION coating agents are silica materials, small organic molecules, biological molecules, and natural and synthetic polymers. A common strategy used for surface modification is the formation of a silica shell, for which alkoxysilane molecules or tetraethyl orthosilicate are generally used [15]. The advantage of a silica coating is that silane groups can be covalently bound onto the NPs' surface through the reaction of the hydroxyl group present on the iron oxide surface and the alkoxysilane functions (–Si-O-R, where R is commonly $-CH_3$ or $-CH_2$-CH_3) [16]. A subsequent crosslinking induces the formation of a silica layer around the particles. Accumulation of PEGylated silane-coated magnetic iron oxide NPs in murine tumors has been reported [17]. Aminosilane-coated SPIONs have demonstrated enhanced cellular uptake and lower toxicity in several cell lines, compared to SiO_2-coated, dextran-coated or naked SPIONs [18]. Moreover, surface modification with 3-aminopropyltriethoxysilane (APTES) provides a platform for further conjugation of other diagnostic or therapeutic agents to the primary amine groups of APTES. Similarly, gold shells protect against surface oxidation and reduce NPs agglomeration in aqueous solution [19]. They also increase the biocompatibility of SPIONs by inhibiting the formation of hydroxyl radicals and reactive oxygen species (ROS).

Small organic molecules are frequently used for stabilizing magnetic NPs. This is generally achieved by carboxylates, phosphates and sulfates, due to their high affinity for iron oxide surfaces. These strong interactions result in an ionic attraction between the acidic functions of the coating agents and the hydroxyl groups of NPs (Fe atoms coordinate with water in aqueous solutions. A hydroxyl-functionalized iron oxide surface results from the subsequent dissociation of water. Since hydroxyl groups are amphoteric, they react with acids and bases [20]). Among carboxylic acids, citric and dimercaptosuccinic acids are the most commonly used [21,22]. These polyacids contribute to a stable colloidal suspension, resulting from their high coordination on metal surface. Unfortunately, the ionic bonds between the carboxylic functions and the iron oxide surface are labile and can be easily broken by the elevation of temperature or by carboxylic compounds presenting a higher affinity to the surface. Phosphate and phosphonate derivatives are also promising stabilizing candidates, which are stably adsorbed on the metal surface and are capable of forming a strong interaction in aqueous solution. Stabilization by biological molecules is not a common strategy and involves the application of proteins such as avidin–biotin [23] or human serum albumin [24]. Natural and synthetic polymer coatings render NPs' biocompatibility and improve their blood circulation times. Besides, surface functional groups (e.g., carboxylic acids, amines, thiols, etc.) of polymers can facilitate the conjugation of therapeutic, diagnostic and/or targeting ligands. Dextran is a natural polymer widely used for coating of iron-oxide NPs due to its biocompatibility and biodegradability [25]. This polysaccharide can be strongly absorbed on the NPs' surface through the strong hydrogen bonds formed between the hydroxyl groups present on the polymer chains and the surface of iron oxide cores [26]. Several preclinical MRI contrast agents have been produced with a dextran coating or dextran derivatives such as carboxydextran and carboxymethyl dextran [27]. Although dextran is a favorable natural polymer, other polymers such as chitosan, gelatin, alginate and pullulan can also be used as stabilizing agents. Another natural and biodegradable polymer is polylactic acid that can be used for the preparation of stable colloid suspensions with a typical hydrodynamic diameter of 10 – 180 nm [28].

PEG is the most widely used synthetic biocompatible polymer for coating of nanoscale DDSs. PEGylation improves the blood circulation time, hydrophilicity and biocompatibility of nanocarriers. Further, PEG may be coupled with other polymers to increase the hydrophilic properties of nanocarriers [29]. Polymeric magnetic micelles composed of poly(ε-caprolactone)-β-PEG copolymers surrounding the SPION core have shown an increase of r_2 relaxivities and image contrast in MRI [30]. Other synthetic polymers used for coating magnetic NPs include but are not limited to polyvinyl alcohol (PVA) [31], polystyrene [32], polyvinylpyrrolidone [33], polyacrylic acid (PAA) [34], polyethylenimine [35] and a variety of their copolymers.

Polymeric coatings improve the SPIONs' pharmacokinetic profile, while also tailoring drug loading and release behavior. The coating of SPIONs can be performed via several approaches, including *in situ* coating, post-synthesis adsorption or post-synthesis grafting. The first two methods form a coating that uniformly encapsulates the NP core, whereas in post-synthesis grafting method polymer end-groups are anchored to the NP's surface, forming brush-like extensions.

Coating is a major determinant of SPION stability in solution and physiological media. The stability of Fe_3O_4 NPs is compromised in ambient conditions through oxidation to Fe_2O_3 or dissolution in acidic media (this is why the synthesis of Fe_3O_4 NPs is performed in anaerobic conditions). On the contrary, Fe_2O_3 NPs are chemically stable in alkaline or acidic environments [36]. Further, oxidation of

magnetic NPs by ROS results in loss of magnetic properties. Grafting or coating is used for increasing the stability of SPIONs. But, when nonmagnetic materials are used for coating SPIONs, a decrease in saturation magnetization may occur [37].

The presence of salts in the solution promotes the aggregation of colloidal SPIONs by neutralization of surface charges [38,39]. Although the presence of trace amounts of the organic acids destabilizes the magnetite dispersion, a high concentration of organic acids improves colloidal (electrostatic) stability and salt tolerance of magnetic dispersion by masking the original surface properties of magnetite and overcharging of NPs [40]. Thus, salt-induced aggregation of SPIONs can be inhibited by the addition of organic acids or surfactants to the solution [41]. Further, in colloidal solutions, aggregation of SPIONs is observed due to their extremely large surface-to-volume ratio and a large surface energy with magnetic and long-range attractive van der Waals forces [42]. Therefore, the colloidal stability of SPIONs is dependent on the nature of coating as well as environmental conditions such as ionic strength, pH and specific properties of cell culture media [39,43].

Other than increasing blood circulation time through coatings which leads to more available concentration of NPs to target the tissue of interest, active accumulation of SPIONs in the targeted site can be enhanced by surface engineering with cell-recognizing vector molecules, including monoclonal antibodies and antibody fragments against cell surface receptors (e.g., HER2/Neu, myosin, lymphocyte, selectin, V-CAM1, etc.), lectins (carbohydrate-binding proteins), transferrin, saccharides (hyaluronic acid, etc.), hormones, folate and vitamins (e.g., thiamine and B_{12}). Surface functionalization with targeting moieties can increase the efficiency of drug-loaded nanoscale DDS in reaching the target regions and can decrease the side effects associated with unintended systemic delivery of drugs to non-targeted organs. For example, Huh *et al.* [44] modified magnetic nanocrystals with cancer-targeting antibody herceptin and used these bioconjugates as MRI probes for *in vivo* monitoring of human cancer cells implanted in live mice. Further functionalization of these nanocrystal probes with fluorescent dye-labeled antibodies allows for simultaneous *in vitro* and *ex vivo* optical detection of cancer as well as *in vivo* MRI.

Further, functionalization with certain peptides such as arginine-glycine-aspartic acid (RGD) and luteinizing hormone releasing hormone can enhance the intracellular delivery of SPIONs. For example, RGD conjugation has been shown to enhance the targeting efficiency and the uptake of ultra-small SPIONs coated with 3-aminopropyltrimethoxysilane (APTMS) by human umbilical vein endothelial cells (HUVEC) cells [45]. The engineered NPs could label $\alpha_v\beta_3$ integrins expressed on HUVEC cells. Further, *in vivo* studies using a clinical 1.5T MR scanner demonstrated the capability of these MRI probes in distinguishing tumors with differential $\alpha_v\beta_3$ integrin expression. Functional molecules used for targeting SPION DDSs along with their drug delivery applications have been presented in **Table 1**.

3. Barriers and considerations in SPION-based drug delivery

Several hindrances compromise the efficiency of DDSs. Physiological barriers, such as vascular epithelium, hinder the access of SPIONs to their cellular targets. In the context of cancer therapy, although DDSs can enhance the accumulation of drug in the target region, it should be noted that only a very small fraction of the total intravenously administered dose is deposited in the tumor [46]. Since intracellular localization takes place only after extravasation and nanoscale DDSs cannot efficiently direct themselves to the target cells even in the presence of surface-engineered functional moieties, research has been focused on enhancing the blood circulation time of DDSs to increase the chance of delivery to the target site by exploiting enhanced permeability and retention (EPR) effect. Exploiting EPR effect in drug delivery relies on the leaky structure of tumor vasculature and poor lymphatic drainage, which enhance the accumulation and retention of NPs in tumor tissue. However, compared to other DDSs, SPIONs take advantage of their magnetic properties that can increase targeting efficiency by applying local external magnetic field. During the delivery of pharmaceuticals and imaging agents to the brain, another problem is the passage through the BBB. Only particles with a sufficiently small size and appropriate physicochemical properties can pass through the BBB. It has been suggested that BBB permeability is influenced by several physicochemical properties [47].

Biodistribution, pharmacokinetics and *in vivo* cellular uptake of SPIONs are directly linked to their physicochemical properties, including hydrodynamic size, charge, shape, surface and the nature of coating material (**Figure 1**) [48]. For example, hydrodynamic size influences the NPs' concentration in blood and affects their clearance from circulation [49]. The ideal size of nanoparticulate DDS is suggested to be between 10 and 100 nm, since at that size they can avoid uptake by RES [50]. The size of the particles plays a crucial role in tissue penetration; more specifically, smaller NPs provide higher effective surface area for ligand attachment, higher stability in suspension and, consequently, higher diffusion rate in tissues [2]. Particle size is also important in optimal exploitation of the EPR effect. Particularly in drug delivery with SPIONs, the magnetism is size-dependent. The charge and hydrophobicity of NPs influence their biodistribution by interactions of the NPs with plasma proteins, the immune system, extracellular matrices or non-targeted cells. A recent study has indicated that coating is even more important than size in terms of cellular uptake of SPIONs and ultra-small SPIONs [51]. Hydrophobic NPs have short circulation half-life due to the adsorption of plasma proteins to their surface, which can lead to recognition by the RES, eventuating in opsonization and removal from circulation [52]. Surface modification with molecules like the hydrophilic PEG has been

Table 1. Functionalized superparamagnetic iron oxide nanoparticles used for drug delivery applications and preclinical studies.

Functional molecules	Structure of DDS	*In vitro*/*in vivo*	Application	Results	Ref.
Folate	Folate-conjugated rhodamine isothiocyanate/*o*-carboxymethyl chitosan/SPIONs	*In vitro*, folate receptor overexpressing HeLa and normal L929 fibroblast cells	MRI and drug delivery to cervical cancer	Higher accumulation of NPs in cells overexpressing the human folate receptor, potential for MRI	[127]
Folate	R (folate or methoxy)-PEG_{114}-P (Glu-Hyd-doxorubicin)-PEG_{46}-acrylate)	*In vitro*, HeLa cell line	MRI and drug delivery to cervical cancer	Much higher r_2 relaxivity value than commercial Feridex and significant cytotoxicity	[105]
Folate	Folate-conjugated magnetic NPs	*In vitro*, folate receptor positive HeLa cells	Cervical cancer targeting	Higher accumulation of NPs in cells overexpressing the human folate receptor	[128]
Folate	Folate-conjugated maghemite NPs	*In vitro*	Intracellular hyperthermia treatment of solid tumors	Higher accumulation of NPs in cells overexpressing the human folate receptor	[129]
Folate	Folate-conjugated SPIONs–polymeric (copolymer methyl methacrylate and PEG methacrylate) micelle hybrids	*In vitro*, HeLa cells	MRI and drug delivery to cervical cancer	Very good contrast enhancement	[130]
Folate	Folate-functionalized polymeric micelles (PEG-block-poly[ε-caprolactone]) loaded with SPIONs and sorafenib	*In vitro*, HepG2 cells	Drug delivery to human hepatic carcinoma	Higher internalization of targeted micelles, significant cytotoxicity	[131]
Folate	Folate-conjugated PEG-modified SPIONs containing doxorubicin	*In vitro*, MCF-7 cancer cells	MR and fluorescence imaging, targeted drug delivery and hyperthermia effect for breast cancer	Increased particle uptake compared to non-targeted particles	[132]
Folate	Poly (ethylene oxide)-trimellitic anhydride chloride-folate doxorubicin and SPIONs-folate	*In vivo*, rats and rabbits	Simultaneous MRI and drug delivery to liver cancer	Anticancer efficacy and specific targeting of folate receptor-expressing tumors; the relative tumor volume was decreased two- and four-fold compared with the free drug and DOXIL® groups in the rat and rabbit models, respectively; formulation showed higher MRI sensitivity comparable to the commercial Resovist®	[133]

APTES: 3-Aminopropyltriethoxysilane; cRGD: Cyclic arginine–glycine–aspartic acid; DDS: Drug delivery systems; GFP: Green fluorescent protein; HepG2: Hepatocellular carcinoma cells; LHRH: Luteinizing hormone releasing hormone; MMC: Mouse mammary carcinoma; NPs: Nanoparticles; PEI: Polyethylenimine; PLGA: Poly(lactic-*co*-glycolic acid); PSMA: Prostate-specific membrane antigen; RGD: Arginine-glycine-aspartic acid; RES: Reticuloendothelial system; scAbCD3: CD3 single chain antibody; siRNA: Small interfering RNA; SPIONs: Superparamagnetic iron oxide nanoparticles; TfRscFv: Transferrin receptor single-chain antibody fragment.

Table 1. Functionalized superparamagnetic iron oxide nanoparticles used for drug delivery applications and preclinical studies (continued).

Functional molecules	Structure of DDS	*In vitro*/*in vivo*	Application	Results	Ref.
Folate	SPION cores coated with a mixture of the triblock copolymer methoxy PEG-*b*-poly (methacrylic acid-*co*-*n*-butyl methacrylate)-*b*-poly(glycerol monomethacrylate) and the folate-conjugated block copolymer folate-PEG-*b*-poly (glycerol monomethacrylate) loaded with doxorubicin	*In vitro*, HeLa cells	Drug delivery to cervical cancer	Targeting strategy enhanced NP uptake and cytotoxicity	[134]
Folate	Folate-iron oxide incorporated into Pluronic® F127 micelles	*In vitro*, KB mouth epidermal carcinoma cells	MRI and drug delivery	Higher intracellular uptake into KB cells	[135]
Methotrexate targeting folate receptor	Iron oxide NPs modified with APTES and covalently bound with methotrexate (drug release in low pH of the lysosomes)	*In vitro*, MCF-7 and HeLa cells	Imaging and therapy of breast and cervical tumors	Higher uptake of targeted NPs in cells with folate receptor	[136]
Methotrexate	Methotrexate immobilized on iron oxide NP surface via a PEG self-assembled monolayer	*In vitro*, 9L glioma cells,	Real-time monitoring of drug delivery to brain tumors through MRI	Higher uptake of targeted NPs, significant contrast enhancement, higher cytotoxicity than free methotrexate *in vitro*	[137]
LHRH	SPIONs- poly(propyleneimine) generation 5 dendrimer–siRNA complex coated with PEG and LHRH	*In vitro*	Drug delivery	Enhanced internalization into cancer cells and increased efficiency of gene suppression *in vitro*	[138]
LHRH	LHRH-conjugated SPIONs	*In vitro* and *in vivo*	Drug delivery to tumors and metastases from human breast cancer	Targeted NPs had a 12-fold higher accumulation than bare NPs *in vitro*, higher accumulation in breast to lung metastases *in vivo*	[139]
Murine melanoma antigens, hgp10025–33	SPIONs carrying murine melanoma antigens, hgp10025–33	*In vivo*, mouse model	Antigen delivery to murine melanoma	Efficient uptake of engineered NPs	[140]
Anti-PSMA antigen	Quantum dots conjugated onto the surface of a nanocomposite consisting of a spherical PS matrix and the internally embedded, high fraction of SPIONs + PLGA + paclitaxel load	*In vitro*, PC3mm2 and LNCaP prostate cancer cells, *in vivo*, tumor-bearing nude mice	Drug storage, targeting and imaging of prostate cancer	Considerable targeting	[141] [142]

APTES: 3-Aminopropyltriethoxysilane; cRGD: Cyclic arginine–glycine–aspartic acid; DDS: Drug delivery systems; GFP: Green fluorescent protein; HepG2: Hepatocellular carcinoma cells; LHRH: Luteinizing hormone releasing hormone; MMC: Mouse mammary carcinoma; NPs: Nanoparticles; PEI: Polyethylenimine; PLGA: Poly(lactic-*co*-glycolic acid); PSMA: Prostate-specific membrane antigen; RGD: Arginine-glycine-aspartic acid; RES: Reticuloendothelial system; scAbCD3: CD3 single chain antibody; siRNA: Small interfering RNA; SPIONs: Superparamagnetic iron oxide nanoparticles; TfRscFv: Transferrin receptor single-chain antibody fragment.

Table 1. Functionalized superparamagnetic iron oxide nanoparticles used for drug delivery applications and preclinical studies (continued).

Functional molecules	Structure of DDS	*In vitro*/*in vivo*	Application	Results	Ref.
Hyaluronan against CD44	Hyaluronan-coated SPIONs + doxorubicin	*In vitro,* SKOV and NCI/ADR-RES cells	Targeted delivery as well as MR and fluorescence imaging of ovarian carcinoma	Higher uptake of targeted NPs compared to non-targeted NPs, doxorubicin-based DDS killed not only drug-sensitive but also multidrug-resistant cancer cells	
cRGD peptide	Peptide-conjugated thermally crosslinked SPIONs loaded with doxorubicin	*In vitro,* U87MG cells	MRI and drug delivery to human glioblastoma	High preferential binding to U87MG, integrin $\alpha_v\beta_3^+$	[143]
RGD	RGD-modified PEG-grafted PEI functionalized with SPIONs	*In vitro*, human hepatocellular carcinoma cell line Bel-7402, *in vivo*, nude mice Bel-7402 hepatoma model	MRI-visible siRNA delivery to hepatocellular carcinoma	High transfection efficiency of targeted NPs versus non-targeted NPs, significant gene suppression, inhibition of tumor growth in the animal model	[144]
cRGD	cRGD-functionalized, doxorubicin and macrocyclic 1,4,7-triazacyclononane-*N*, *N*′, *N*″-triacetic acid-conjugated and ^{64}Cu-labeled PEG-SPIONs	*In vitro,* U87MG cells, *in vivo*, female athymic nude mice	Drug delivery and PET/MRI of human glioblastoma (tumors with integrin $\alpha_v\beta_3$ expression)	Higher level of cellular uptake, higher cytotoxicity, similar MRI r_2 relaxivity of the SPIONs to that of the commercial Feridex	[145]
γ-amino-proline-derived cell penetrating peptide	Peptide-conjugated SPIONs	*In vitro*, HeLa cells	Drug delivery to cervical cancer	Higher internalization compared to TAT–SPIONs conjugate	[146]
Chlorotoxin peptide targeting MMP-2	Iron oxide NPs conjugated to both methotrexate and chlorotoxin, through a PEG linker	*In vitro*, 9L cells, *in vivo*, 9L flank xenograft tumors in athymic (nu/nu) mice	Imaging and therapy of brain tumors	Preferential accumulation of targeted NPs and increased cytotoxicity in tumor cells	[147]
Chlorotoxin	Iron oxide NPs core conjugated with an amine-functionalized PEG silane and chlorotoxin	*In vitro*, C6 rat glioma cells	MRI-visible drug delivery to brain tumor (and potential for treatment of a variety of cancers overexpressing MMP-2)	Targeted NPs enhanced cellular uptake and caused an invasion inhibition rate of ~ 98% compared to unbound NPs (~ 45%).	[148]
Chlorotoxin	SPIONs coated with PEG-grafted chitosan and PEI	*In vitro*, C6 rat glioma cells	siRNA delivery to brain glioma and noninvasive monitoring through MRI	Receptor-mediated cellular internalization of nanovectors and enhanced gene knockdown, contrast enhancement for MRI	[149]
Chlorotoxin	Iron oxide NP core coated with a copolymer of chitosan, PEG and PEI. GFP encoding DNA was bound to these NPs, and chlorotoxin was then attached using a short PEG linker	*In vivo*, intravenous injection to mice bearing C6 xenograft tumors	MRI-visible gene delivery to brain glioma	Chlorotoxin did not affect the accumulation of NPs at the tumor site, but specifically enhanced their uptake into cancer cells	[150]

APTES: 3-Aminopropyltriethoxysilane; cRGD: Cyclic arginine–glycine–aspartic acid; DDS: Drug delivery systems; GFP: Green fluorescent protein; HepG2: Hepatocellular carcinoma cells; LHRH: Luteinizing hormone releasing hormone; MMC: Mouse mammary carcinoma; NPs: Nanoparticles; PEI: Polyethylenimine; PLGA: Poly(lactic-*co*-glycolic acid); PSMA: Prostate-specific membrane antigen; RGD: Arginine-glycine-aspartic acid; RES: Reticuloendothelial system; scAbCD3: CD3 single chain antibody; siRNA: Small interfering RNA; SPIONs: Superparamagnetic iron oxide nanoparticles; TfRscFv: Transferrin receptor single-chain antibody fragment.

Table 1. Functionalized superparamagnetic iron oxide nanoparticles used for drug delivery applications and preclinical studies (continued).

Functional molecules	Structure of DDS	*In vitro*/*in vivo*	Application	Results	Ref.
EPPT peptide that specifically targets uMUC-1	Magnetic NP-EPPT-siRNA	*In vivo*, intravenous delivery into subcutaneous mouse models of breast cancer	MRI-guided siRNA delivery to breast adenocarcinoma	Significant gene downregulation after preferential tumor uptake, significant decrease in tumor growth rate	[151]
CG-rich duplex containing PSMA aptamer	Doxorubicin/aptamer-conjugated thermally crosslinked SPIONs	*In vitro and in vivo*, LNCaP cells	MRI and drug delivery to prostate tumor tissue	Selective drug-delivery efficacy in the LNCaP xenograft mouse model	[152]
A10 RNA aptamer which binds the extracellular domain of the PSMA	N-terminated A10 aptamer, thermally crosslinked SPIONs coated with a carboxylic acid-PEG-derived, anti-biofouling polymer, and doxorubicin which is intercalated in the aptamer and complexed with the SPIONs through charge interactions	*In vitro*, LNCaP and PC3 cells	Drug delivery and MRI of prostate cancer	High uptake by PSMA-expressing PCa cells (LNCaP), highly sensitive MRI, high cytotoxicity of doxorubicin	[153]
A10 RNA aptamer targeting PSMA (+) cells and a DUP-1 peptide aptamer specific to PSMA (-) cells	A10 RNA-DUP-1 conjugated by streptavidin, doxorubicin-loaded onto the stem region of the A10 aptamer and aptamers were loaded on SPIONs	*In vitro*, LNCaP, PC3, HeLa, SW620, MCF-7 and PNT2 cell lines	Drug delivery to prostate cancer	Doxorubicin delivery to both PSMA (+) and PSMA (-) cells and eventual induction of apoptosis, selective cell uptake of SPIONs and effective drug delivery	[154]
Rotavirus capsid surface protein VP4	VP4-coated Fe_3O_4 NPs loaded with doxorubicin	*In vitro*, HepG2 cells	MR and fluorescence imaging and drug delivery of human hepatic carcinoma	Improved MRI sensitivity compared with dextran- and bovine serum albumin -coated Fe_3O_4 NPs, significant cytotoxicity	[155]
scAbCD3	scAbCD3-PEG-grafted PEI complexed with SPIONs further condensed with plasmid DNA	*In vitro*, HB8521 cells, a rat T-lymphocyte line	MRI-visible gene delivery for immunosuppression	16-fold enhancement in the gene transfection level, effective T-cell anergy induced by gene therapy	[156]
Anti-TfRscFv	Liposome (DOTAP-DOPE)–SPIONs complex functionalized with TfRscFv	*In vitro*, human pancreatic (PANC-1) and MDA-MB-231 breast cancer cell lines, *in vivo*, female athymic nude (nu/nu) mice injected with PANC-1 cells (bearing pancreatic tumors)	Drug delivery to pancreatic cancer	Encapsulation in liposomes resulted in 11-fold increase in SPIONs' uptake in cancer cells *in vitro*; specific and efficient delivery of SPIONs into tumor cells after systemic administration	[157]

APTES: 3-Aminopropyltriethoxysilane; cRGD: Cyclic arginine–glycine–aspartic acid; DDS: Drug delivery systems; GFP: Green fluorescent protein; HepG2: Hepatocellular carcinoma cells; LHRH: Luteinizing hormone releasing hormone; MMC: Mouse mammary carcinoma; NPs: Nanoparticles; PEI: Polyethylenimine; PLGA: Poly(lactic-*co*-glycolic acid); PSMA: Prostate-specific membrane antigen; RGD: Arginine-glycine-aspartic acid; RES: Reticuloendothelial system; scAbCD3: CD3 single chain antibody; siRNA: Small interfering RNA; SPIONs: Superparamagnetic iron oxide nanoparticles; TfRscFv: Transferrin receptor single-chain antibody fragment.

Table 1. Functionalized superparamagnetic iron oxide nanoparticles used for drug delivery applications and preclinical studies (continued).

Functional molecules	Structure of DDS	*In vitro*/*in vivo*	Application	Results	Ref.
Transferrin	Transferrin-conjugated SPIONs	*In vivo*, C6 glioma rat model	Targeting and imaging of brain glial tumors	Significant contrast enhancement	[158]
Hepama-1 humanized monoclonal antibody and radioactive rhenium-188	Hepama-1 conjugated SPIONs	*In vitro*, SMMC-7721 liver cancer cells	Drug delivery to liver cancer	Significant cytotoxicity in SMMC-7721 cells	[159]
Antibody HuCC49ΔCH2 and fluorescent dye 5-FAM	HuCC49ΔCH2 and fluorescent dye 5-FAM conjugated to PEG of iron oxide NPs and anticancer drugs doxorubicin, azido-doxorubicin, MI-219 and 17-DMAG were encapsulated into iron oxide NPs	*In vitro*, LS174T colon cancer cell line	MR and fluorescence imaging and pH-dependent intracellular drug release for treatment of colon cancer	HuCC49ΔCH2-fuctionalized SPIONs delivered more drug to LS174T cells than nonspecific IgG-SPIONs	[160]
Monoclonal antibody against the neu receptor	SPIONs coated with a copolymer of chitosan and PEG were labeled with a fluorescent dye and conjugated with monoclonal antibody	*In vivo*, transgenic MMC cells	Drug delivery and MRI of MMC	Anti-neu antibody-conjugated NPs showed high uptake in neu expressing MMC cells compared with IgG-conjugated NPs, significant contrast enhancement	[161]
EGFRvIII antibody	EGFRvIII antibody-conjugated iron oxide NPs	*In vitro*, U87MG cells, *ex vivo*, neurospheres from patients, *in vivo*, athymic nude (nu/nu) mice inoculated with U87ΔEGFRvIII cells	MRI-guided convection-enhanced delivery and targeted therapy of brain glioblastoma	A significant decrease in glioblastoma cell survival, no toxicity in human astrocytes; a significant increase in animal survival rate was found after convection enhanced delivery of magnetic NPs	[162]

APTES: 3-Aminopropyltriethoxysilane; cRGD: Cyclic arginine–glycine–aspartic acid; DDS: Drug delivery systems; GFP: Green fluorescent protein; HepG2: Hepatocellular carcinoma cells; LHRH: Luteinizing hormone releasing hormone; MMC: Mouse mammary carcinoma; NPs: Nanoparticles; PEI: Polyethylenimine; PLGA: Poly(lactic-*co*-glycolic acid); PSMA: Prostate-specific membrane antigen; RGD: Arginine-glycine-aspartic acid; RES: Reticuloendothelial system; scAbCD3: CD3 single chain antibody; siRNA: Small interfering RNA; SPIONs: Superparamagnetic iron oxide nanoparticles; TfRscFv: Transferrin receptor single-chain antibody fragment.

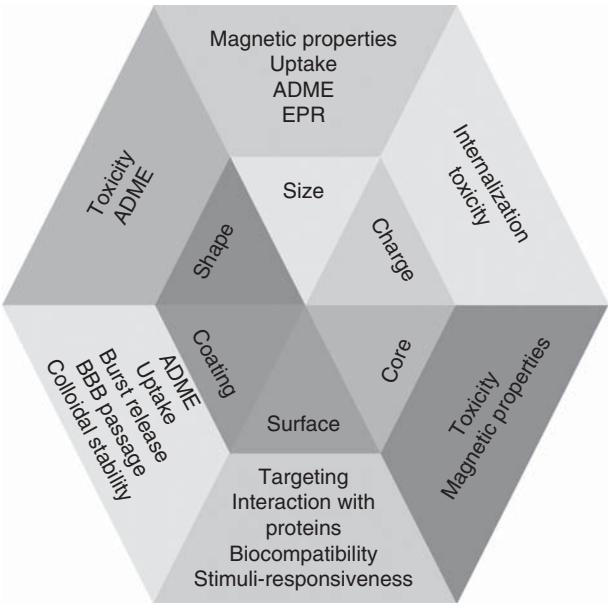

Figure 1. Illustration of the association of the physicochemical properties of superparamagnetic iron oxide nanoparticles with their biological interactions, *in vivo* fate, toxicity, formulation characteristics and targeting efficiency.

shown to reduce NPs' opsonization through steric repulsion. Positively charged NPs can also bind to non-targeted cells and undergo nonspecific internalization. Positively charged SPIONs generally have shown a higher cellular internalization compared to the negatively charged ones [53,54].

Drug delivery using SPIONs suffers from a number of drawbacks. SPION DDSs in which drug molecules are conjugated to the NPs' surface exhibit low drug entrapment efficiency and failure to release the drug molecule at the target site due to covalent binding. Further, residual concentration of catalysts (e.g., Cu) used during the covalent linking of drugs to SPIONs can cause *in vivo* toxicity. Moreover, controlling the orientation of functional moieties to the NP's surface is both important and difficult. For example, when carboxylic acid-functionalized SPIONs interact with ligands with multiple amine groups, inactivation of ligands is observed. SPIONs must possess favorable pharmacokinetic properties. On entry of a DDS to the blood stream, most of the drug payload might be released – an effect called initial burst release. To alleviate this effect in SPIONs, Mahmoudi *et al.* [55] coated iron oxide NPs with crosslinked PEG-co-fumarate, which reduced the burst release of surface-loaded tamoxifen by 21%, compared with the non-coated tamoxifen-loaded particles.

4. Toxicity and biocompatibility of SPIONs

Biocompatibility is an essential factor that must be addressed before SPIONs can be used *in vivo*. In general, SPIONs have only been associated with low toxicity in the human body. Due to the broad safety margin of iron oxide NPs, SPION-based dextran-coated products (Feridex, Endorem, Combidex and Sinerem) are currently approved as MRI contrast agents. Among several other metal oxide NPs, iron oxide demonstrates acceptable safety profile and non-cytotoxicity in concentrations < 100 µg/ml [56]. A study on human glia, breast cancer and normal cell lines indicated that SPIONs with varying physiochemical properties only demonstrate low toxicity or accountable cytotoxicity at doses > 100 µg/ml and are nontoxic at lower doses [57]. Although only a few *in vivo* toxicity assessment studies on humans exist, it has been shown that dextran-coated ultra-fine SPIONs only produce mild and transient side effects, including urticaria, diarrhea and nausea [4,58]. SPIONs are suggested to biodegrade and clear from the body through the endogenous iron metabolic pathway [4]. The released iron is first metabolized in the liver and then either used in production of red blood cells or eliminated from body through kidneys.

In spite of general safety in low concentrations, SPIONs have been shown to arrest the cell cycle in the G0G1 [59]. Further, Mahmoudi *et al.* [60,61] have noted the existence of gas vesicles and increased granularity in SPION-treated cells, which were indicative of autophagy-mediated cytotoxicity. Therefore, thorough characterization of every single formulation seems to be necessary. The biocompatibility extent of SPIONs mainly depends on the nature of the magnetic content, final NP size and nature of coating. The toxicity of SPION-COOH, plain SPIONs and SPION-NH_2 surface chemistries were evaluated by comparing the gene expression profiles of hypertrophic cardiomyopathy human heart, BE-2-C brain and 293T kidney cell lines using DNA microarrays [62]. SPION-COOH was shown to alter the expression of genes involved in cell proliferative responses. Yang *et al.* studied the toxicity of Fe_3O_4 NPs (10 and 100 – 150 nm particles with different functional groups) by quantifying metabolic activity, membrane integrity and DNA stability in normal fibroblasts versus fibrosarcoma cells [63]. Whereas all magnetic NPs exerted almost ≤ 5% cytotoxicity or genotoxicity in fibrosarcoma cells at concentrations < 500 µg/ml, the positively charged APTMS-coated magnetic NPs induced > 10% toxicity against normal cells. Dose, size and surface charge were the most important determinants of magnetic NPs genotoxicity, in which smaller and positively charged (APTMS-coated) magnetic NPs had higher toxicity in normal cells than the cancer cell line.

Another important issue that must be considered is the effects of SPION interactions or metabolism on the iron homeostasis of the human body. Jain *et al.* [64] have studied the changes in serum and tissue iron levels for 3 weeks after administration of magnetic NPs to rats. Although the iron levels in serum gradually increased during the first week, thereafter, levels of iron slowly declined. A greater fraction of the injected iron was shown to localize in the liver and spleen compared with brain, heart, kidney and lung. In another study, the toxicity and pharmacokinetics of SPIONs

was studied in dogs and mice using radioactive iron [65]. About 1 h post-injection, 82.6 and 6.2% of the SPIONs localized in the liver and spleen, respectively. The concentration of particles gradually decreased in the liver and spleen with radioactive iron being incorporated into the hemoglobin of erythrocytes. Interestingly, a previously induced anemia was successfully treated within a period of 7 days. Although no acute or subacute toxic side effects were observed with a maximal dosage of 3000 mmol Fe/kg (i.e., 150 times higher than the concentration used in liver MRI) in dogs and mice, cautionary measures must always be taken. Since free iron is toxic [66], the iron dose of the clinically administered SPIONs must be many times lower than body iron levels. In normal circumstances, the injected iron is expected to be metabolized and regulated by normal physiological iron homeostatic mechanisms. Evidently, repeated dosing of SPIONs in short intervals would not be a desirable option in imaging and drug delivery. FDA may not approve the application of the SPION-based products in patients with iron metabolism problems.

5. Protein corona as a newly discovered barrier/promise in drug delivery

On entering the blood stream, NPs are rapidly covered with a protein corona composed of two layers of high-affinity and low-affinity proteins. The protein corona composition depends on the physicochemical properties of NPs [67] as well as interaction temperature [68], protein source [69], incubation time with protein source [67], concentration of protein source [70] and gradient concentration [71]. The adsorption of proteins onto the NP surface has been shown to negate the effects of functional moieties and mask the targeting efficiency of the nanoscale DDSs by up to 99% [72,73]. In addition, adsorption of proteins facilitates the uptake and elimination of NPs by RES, leading to decrease in targeting efficacy [74,75]. Protein corona might also allow NPs to enter unintended and otherwise inaccessible tissue sites [76,77]. Very recently, we showed that the protein corona can change the relaxivity of the SPIONs with various surface charges [78]. More specifically, it was revealed that the protein corona considerably decreased the relaxivity of the positively charged SPIONs but had a slight and no effect on the relaxivity of negative and plain SPIONs, respectively. The dramatic decline in the relaxivity of the positively charged SPIONs results from particle agglomeration in the presence of the proteins.

Protein corona brings about a new concern for nanotoxicology. Research has shown that the NP–protein interface has the ability to induce conformational changes in the structure of attached proteins [79]. Following detachment of proteins from the NP surface, changed proteins might induce immunoallergic responses in the blood or protein fibrillation in the intracellular environment and finally lead to neurodegenerative diseases and cancer [80]. Thus, the abovementioned factors are accounted as barriers introduced by protein corona in the field of nanoparticulate drug delivery. To eliminate the negative effects of protein corona on the targeting efficiency of nanocarriers, it has been suggested that the NP surface be coated with hydrophilic antibiofouling polymers, including PEG [81], poly(TMSMA-r-PEGMA) [82], Zwitterions [83] and the like.

On the contrary, protein corona is showing some promise in some aspects of drug delivery. The binding of blood proteins to nanomaterials may reduce cytotoxicity [84] and improve NPs' stability under harsh environmental conditions [85], and the recent attempts have focused on exploiting protein corona for good. For example, coronas on a gold nanorod coated with cetyltrimethylammonium bromide were exploited for holding therapeutics at a capacity of 5 – 10 times higher than that achieved by covalent conjugation. Subsequent release of therapeutics could be achieved either by ultrafast laser excitation of the nanorods at their longitudinal surface plasmon resonance or by increasing the temperature [86]. In another study, DNA payloads were loaded on protein coronas formed around gold nanorods, nanobones and carbon nanotubes. The authors demonstrated that changing the corona composition (especially the concentration of human serum albumin) can tune the DNA release profile from NP protein coronas [87]. Another study demonstrated that, when exposed to plasma, vitronectin molecules coat the lipid particles made of 1,2-dioleoyl-3-trimethylammonium propane and DNA and promote particle uptake in cancer cells expressing high levels of the vitronectin $\alpha_v\beta_3$ integrin receptor [88]. Therefore, rational engineering and fine-tuning of NP's surface might create the opportunity to exploit protein corona for overcoming biological barriers (e.g., vascular or cellular barrier, BBB), or mitigate the toxicity of nanocarriers *in vivo*. For example, although binding of complement protein C3 and opsonizing protein IgG onto NPs promotes their phagocytosis [89], surface adsorption of human serum albumin increases blood circulation time of NPs [90]. Further, it can be speculated to find protein molecules in some surface-modified NPs, which after sorption to NPs surface may direct them to a desired target inside the body.

6. SPION-based drug delivery

SPIONs are nanoscale systems with promising applications in the delivery of chemotherapeutics, genes, peptides, radionuclides and anti-inflammatory agents. Further, the capability of SPIONs in the production of localized heat can be used in magnetic hyperthermia to eradicate cancer cells (**Figure 2**). The mission of a DDS is to deliver the effective concentration of a drug to a desired location inside the body, without undesirable interactions with blood, cells and proteins. Moreover, these nanosystems can be engineered to provide controlled release of the encapsulants either in a time- or stimuli-responsive manner. Most drug delivery studies have been directed to the treatment of cancer. Treatment of solid and malignant tumors is a challenge that is complicated by low drug internalization due to a hard-to-penetrate

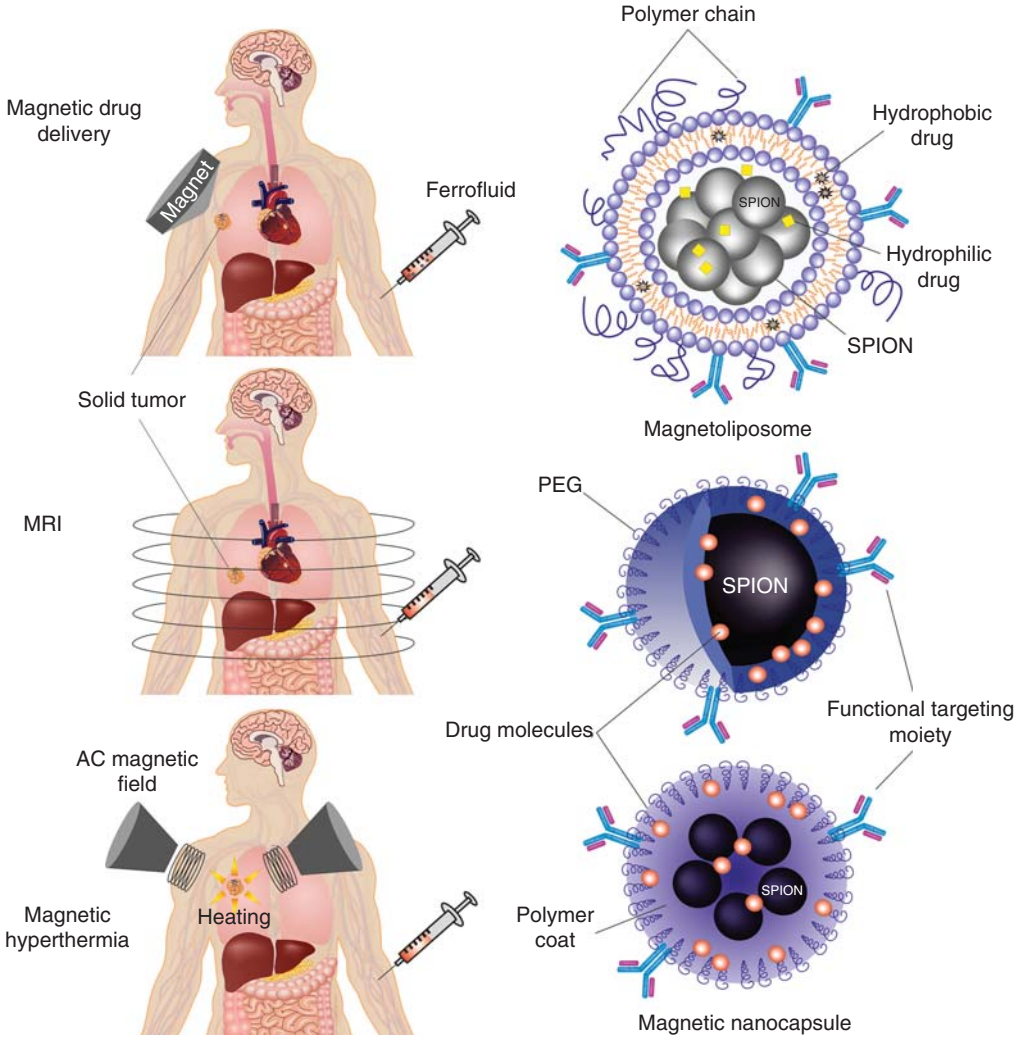

Figure 2. Superparamagnetic iron oxide nanoparticles can be guided to their site of action using an externally applied magnetic field. The subsequent accumulation of superparamagnetic iron oxide nanoparticles in the target site can be exploited for simultaneous drug delivery, MR imaging or hyperthermia therapy of cancer. Magnetoliposomes are composed of a lipid bilayer surrounding superparamagnetic iron oxide nanoparticles and can harbor both hydrophilic and hydrophobic drug molecules in the core or within the lipidic bilayer, respectively. Magnetic capsules containing a single or multi-superparamagnetic iron oxide nanoparticle core are most extensively used, in which drug molecules are usually contained in the polymeric coating. Superparamagnetic iron oxide nanoparticle drug delivery systems are surface engineered with polymers and functional moieties to improve stability and modulate targeting efficiency.

peritumoral endothelium, dense extracellular matrix of solid tumors and the target cell membrane. The selective delivery of therapeutic agents into a tumor enhances their antitumor efficacy and decreases toxicity in normal tissues. Utilizing the EPR effect, a drug-loaded DDS can achieve a higher concentration of a certain drug in a solid tumor than the free drug. In addition, functional tumor-targeted NPs may further increase the local concentration of the drug or change the intracellular biodistribution within the tumor via receptor-mediated internalization. Numerous systems in the nanoscale can be used as advanced DDSs, including micelles, liposomes, polymersomes, NPs, dendrimers or polymers. SPIONs are considered efficient nanovectors since they provide an additional targeting capability; that is, post-injection, the SPION–drug complex can be transported by blood circulation and made to accumulate in the tumor region by applying a magnetic field on the target site. Moreover, MRI can be used simultaneously to validate the localization of magnetic DDSs. When delivered to the target site, the loaded drugs are usually released by diffusion, vehicle rupture or dissolution, endocytosis of the conjugate and final endosomal rupture, as well as smart pH or temperature-sensitive dissociation. The drug is generally coupled to NPs' surface by covalent or ionic bonds. To release the drug in the target

site, the link between the magnetic core and the drug must be cleaved. The link cleavage can be triggered by external stimuli such as variations in pH, temperature or enzymatic reactions.

SPIONs used for drug delivery purposes can be roughly divided in two classes according to their structures: i) nanocapsules with SPIONs in the core; and ii) a porous biocompatible polymer harboring precipitated SPIONs in the pores. Drug molecules are either bound to the NPs' surface or contained within magnetic liposomes and microspheres. Thus, SPION DDSs can be in the form of NPs, nanospheres (nanocapsules), liposomes and microspheres. The efficacy of magnetic drug delivery is associated with a number of physical parameters other than the production and design of the DDS, including field strength and gradient as well as the volumetric and magnetic properties of SPIONs. A strong permanent magnet is commonly fixed outside the body on the desired targeted site to generate the magnetic field gradient. Some researchers have even attempted the implantation of magnets at the pathological site *in vivo* [91].

Developing successful DDSs based on SPIONs has come a long way. Widder *et al.* [92] devised the first magnetically responsive microspheres, in which doxorubicin was encapsulated in albumin magnetic NPs. Later preclinical and clinical studies focused on the intravenous injection of SPIONs at proximity of the tumor site in 14 patients [93,94]. MR tomographic techniques, pharmacokinetic studies and the histological detection of magnetite revealed that in 50% of those patients the ferrofluid could be successfully directed to the tumor sites. Widder *et al.* [95] injected doxorubicin-loaded magnetic albumin intra-arterially proximal to the tumor site in rats bearing Yoshida sarcoma. This increased the targeting yield by 200 times compared to intravenous injection and led to tumor remission.

Nanocapsules have been proved as effective tools for increasing the functionality of magnetic NPs. In fact, the flexibility of using different methods for the preparation, a wide variety of raw materials for preparation, adjustable physicochemical properties (e.g., size, surface charge, morphology, shell thickness, etc.) and functional versatility of nanocapsules have made them promising candidates for biomedical applications. However, given the continuing progress in the field of drug delivery, relevant parameters such as colloidal stability, encapsulation efficiency, release kinetics and interactions at the nano–bio interface (e.g., with proteins) should be thoroughly studied. Nanoencapsulation can not only protect the encapsulated drugs against degradation by pH and light, but it can also minimize tissue irritation and provide controlled release by external features such as temperature, reduction, light radiation and pH changes [96].

Kong *et al.* [97,98] produced hollow silica nanocapsules containing embedded magnetic NPs of Fe_3O_4. The *in vitro* treatment of MT2 breast cancer cells and B16/BL6 mouse melanoma cells with radiofrequency-activated nanocapsules containing camptothecin resulted in significant suppression of cancer and/or tumor growth. It was hypothesized that the remote radiofrequency magnetic field heats up the magnetic NPs and rises the localized liquid temperature inside the nanocapsules. More importantly, a significant increase (6 – 13 times) in the magnetic moment in nanocapsules was observed, as compared to the isolated 10 nm Fe_3O_4 NPs. *In vivo* mouse tumor penetration study using magnetic-guided nanocapsules revealed that the average number of magnetic nanocapsules trapped in the tumor cells was about 200 times higher with magnetic attraction, as compared to that for the control group. Additionally, a moderate magnetic field (~ 1000 Oe) led to the efficient penetration (~ 10 cell layers) of nanocapsules. (**Figure 3** Panel A). In another study, Tan *et al.* [99] reported encapsulation of both conjugated polymers (poly [2-methoxy-5-(2-ethyl-hexyloxy)-1,4-phenylenevinylene]) and magnetic NPs inside a thin silica shell as the fluorescent emitter. *In vitro* MTS (3-[4,5-dimethylthiazol-2-yl]-5-[3-carboxymethoxyphenyl]-2–[4–sulfophenyl]-2H tetrazolium tests) results showed that there is no noticeable cytotoxicity to the human hepatocellular carcinoma cells (HepG2) with nanocapsule concentrations up to 350 mg/ml. Confocal microscopy images of the HepG2 cells cultured under the same conditions demonstrated that, under the influence of an external magnetic field (~ 1.3 T), cellular uptake of nanocapsules was enhanced significantly (**Figure 3** Panel B).

Chitosan has been widely used as a promising gene nanocarrier because of its highly cationic, non-cytotoxic and biodegradable nature [100]. Bae *et al.* [101] synthesized pluronic/chitosan nanocapsules encapsulating iron oxide NPs for magnetically triggered intracellular delivery of various therapeutic agents. The use of an external magnetic field revealed that iron oxide NPs preserved their magnetic property after encapsulation. Intracellular uptake into green fluorescent protein-expressing human lung carcinoma (GFP-A549) showed that, even after 2 h incubation, nanocapsules were not efficiently internalized by cells, whereas in the presence of a magnetic field, they entered cytoplasm only after 30 min. This implies that the magnetic field increases sedimentation of nanocapsules on the cells surface. Kumar *et al.* [102] synthesized chitosan-coated magnetic NPs loaded with plasmid DNA-expressing enhanced green fluorescent protein. The NPs injected into the tail vein of mice could be effectively directed to the heart and kidney via an external magnetic field.

Another strategy employed for magnetic drug targeting and controlled release is to use thermosensitive smart polymers for encapsulation of magnetic NPs. Drug release can be controlled by manipulating the temperature of the polymeric shell (i.e., by swelling and de-swelling), resulting in higher release rates above the lower critical solution temperature (LCST) and lower rates below the LCST. For instance, doxorubicin was incorporated by chemical interaction onto the surface of 3-mercaptopropionic acid hydrazide ($HSCH_2CH_2CONHNH_2$) functionalized magnetic NPs encapsulated with dextran-g-poly(*N*-isopropylacrylamide-*co*-*N*,*N*-dimethylacrylamide) (dextran-*g*-poly(NIPAAm-*co*-DMAAm) as a thermosensitive biodegradable polymer

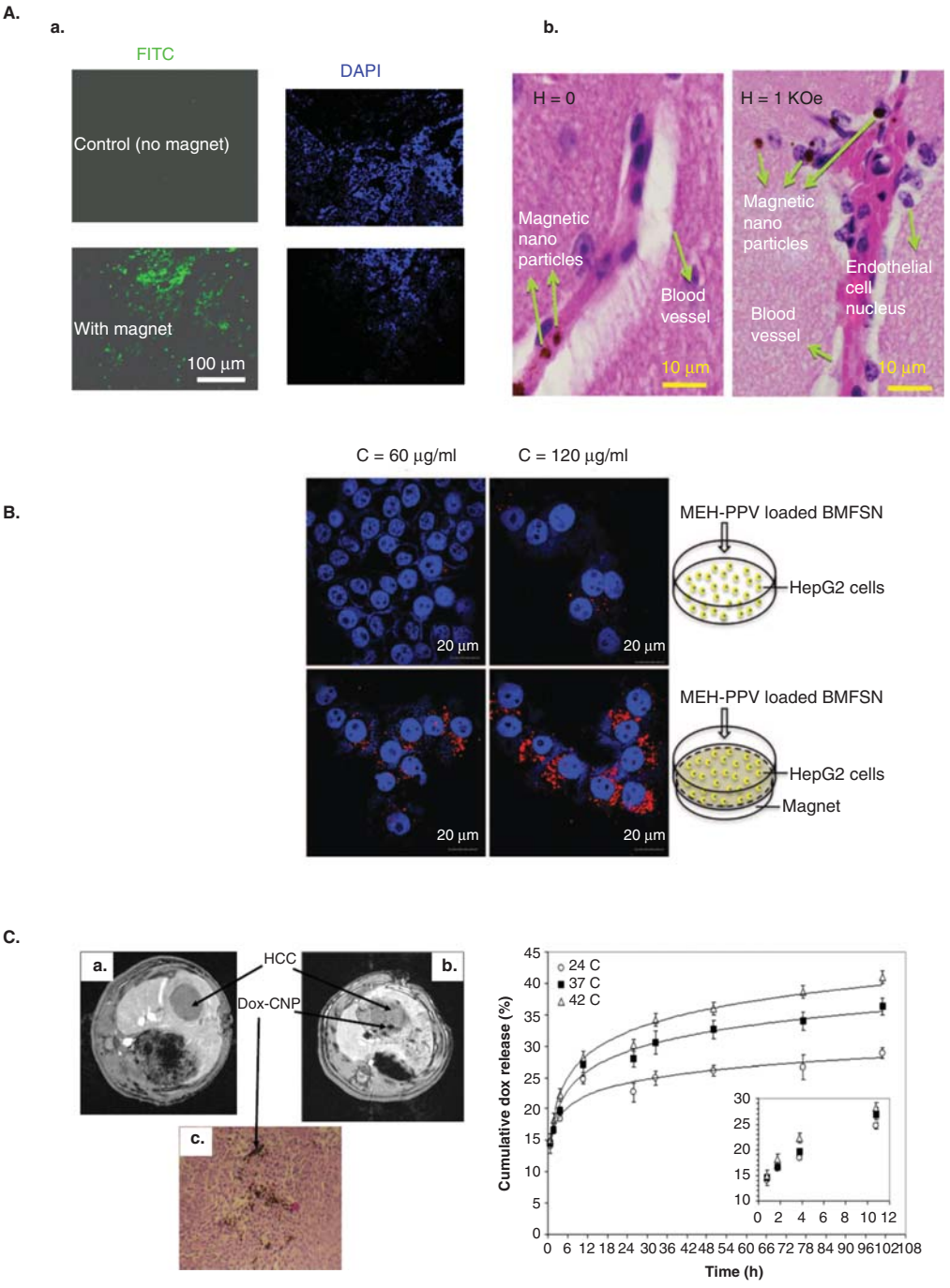

Figure 3. (**A**) (a) FITC imaging results from surgically obtained tumor tissues show the presence of accumulated nanocapsules in the tumor tissue (green markers) when a magnet is placed nearby. The control experiment (i.e., with no magnet nearby) shows very few magnetic nanocapsules near the tumor site. The 4′,6′-diamidino-2-phenylindole images also show the tumor structure via imaging of the nuclei in the tumor. (b) Mouse brain model H&E section imaging is shown. The H&E image represents BBB crossing of magnetic nanocapsules with applied magnetic field. (**B**) Confocal microscopy images of the HepG2 cells cultured with different concentrations of MEH-PPV-loaded nanocapsules without (top) and with (bottom) influence of an external magnetic field are shown. (**C**) MRI scan of the buffalo rat implanted with hepatocellular carcinoma is shown: (a) baseline scan before injection of nanocapsules and (b) 30 min post-injection. Particles are seen as new dark regions in the hepatocellular carcinoma. (c) Histology slide of the hepatocellular carcinoma showing particles as dark deposits. d) *In vitro* drug release profiles of doxorubicin-loaded composite magnetic NPs in phosphate buffer (pH 7.4) at 24°C (T < LCST), 37°C (T > LCST) and 42°C (T > LCST) plotted against time *t* (external magnetic field absent).

A. Adapted with permission from [97,98].

B. Adapted with permission from [99].

C. Adapted with permission from [104].

BBB: Blood brain barrier; FITC: Fluorescein isothiocyanate; H&E: Hematoxylin and eosin stain; HepG2: Hepatocellular carcinoma cells; LCST: Lower critical solution temperature; NP: Nanoparticle; MEH-PPV: Poly [2-methoxy-5-(2-ethyl-hexyloxy)-1,4-phenylenevinylene].

with LCST slightly above 37°C. The drug release from the encapsulated carrier and the bare one in PBS (pH 5.3), at a temperatures of 20°C (< LCST) and a low hyperthermal temperature (i.e., 40°C) (> LCST) was higher from the polymeric shell. At the temperatures lower than LCST, the drug carrier is stable and release is slow, whereas at temperatures higher than LCST the polymeric shell collapses so that the squeezing effect of the polymer leads to enhanced drug release [103]. In another study [104], iron oxide magnetic NPs were encapsulated in thermoresponsive poly-*N*-isopropylacrylamide (LCST ~ 37°C). When the nanocapsules were exposed to an alternating magnetic field (AMF), the release yield of doxorubicin in PBS was in close agreement with the observed release in the absence of an AMF at 42°C, implying the efficiency of using AMF to generate heat for controlled drug release. Additionally, in an *in vivo* experiment, the nanocapsules were successfully targeted to hepatocellular carcinoma by an external magnet in buffalo rat model (**Figure 3** Panel C).

An additional promising approach is to use acid-degradable linkers to attach a drug to the DDS. The linker is degraded in the slightly acidic pH of the tumor microenvironment. Yang *et al.* [105] recently described folate receptor-targeted SPIONs to deliver doxorubicin to tumor cells. SPIONs were encapsulated in the multifunctional polymer vesicles and doxorubicin was conjugated onto the hydrophobic polyglutamate polymer segments via an acid-cleavable hydrazone bond and could be released at low pH values. Due to folate receptor-mediated endocytosis, these NPs showed higher cellular uptake and higher anticancer activity compared to folic acid-free vesicles.

Multifunctional worm-like polymeric vesicles made of heterofunctional triblock polymer R (methoxy or folic acid)-PEG_{114}-PLA_x-PEG_{46}-acrylate harboring SPIONs and doxorubicin were synthesized by Yang *et al.* [106]. Whereas methoxy/folate groups provided tumor targeting at the outer surface, the acrylate groups at the inner surface were cross-linked with free radical polymerization to enhance the stability of particles. Enhanced cytotoxicity in HeLa cell line and higher r_2 relaxivity compared to Feridex®, a commercially available MRI contrast agent, make these magnetic vesicles potential candidates for simultaneous drug delivery and MRI imaging.

In another novel study, Wang *et al.* [107] incorporated SPIONs and doxorubicin into acoustic droplets, which were further functionalized with anti-VEGFR-2 antibody. The VEGFR-2 antibody and magnetism-assisted targeting brought about a 5.4-fold increase in targeting efficacy of the SPION-embedded droplets. The droplets were used effectively to disrupt cells by ultrasound-triggered acoustic droplet vaporization.

Other cargos may also be incorporated into SPIONs formulations. Therapeutic radionuclides such as ^{90}Y, ^{131}I, ^{177}Lu and other α or β emitters can be attached to SPIONs in order to provide a higher local dose of the radioisotope for tumor eradication as compared to conventional radiotherapy. This approach can reduce the associated side effects of radiotherapy. Further, conjugation of diagnostic radiotracers such as ^{67}Ga, ^{64}Cu and ^{99m}Tc to SPION DDSs can also help in tracking the NPs fate *in vivo,* as well as providing opportunity for dual-modality imaging (e.g., MRI/SPECT, MRI/PET). Magnetoliposomes, another class of magnetic DDSs, are nanocomposites of SPIONs surrounded by a phospholipid bilayer with high entrapment efficiency and stability [108]. Further, magnetoliposomes present optimum magnetic responsiveness and can accommodate both hydrophilic and hydrophobic drugs. Moreover, liposomal encapsulation increases the biocompatibility of SPIONs and protects the encapsulants from environmental conditions. Magneto-dendrimers, another subclass, are well-suited nanocomposites for cell tracking using MRI. Further, these systems can couple the two modalities of MR and fluorescent imaging. For instance, dendronized iron oxide NPs have been devised for multimodal imaging [109] and for noninvasive tracking of stem cell transfer for muscle disorders [110].

Magnetic hyperthermia offers the possibility of taking a drug-free approach to the treatment of cancer by localized heating of cancer cells from inside. Raising the intracellular temperature to 41 – 47°C results in cancer cell apoptosis, whereas normal cells can tolerate this temperature. Targeted hyperthermia is based on the endocytic uptake of magnetic NPs followed by their accumulation and concentration in intracellular endosomal vesicles. The subsequent exposure of these NPs to a high frequency AMF heats them up through absorption of the energy and its conversion to heat (magnetic relaxation), leading to the localized killing of the cells. NP size is a determinant factor of heating power. Yallapu *et al.* [111] reported on the synthesis of water-dispersible multifunctional SPIONs suited for hyperthermia, MRI and drug delivery. The magnetic NPs were coated with multilayer β-cyclodextrin and pluronics and were loaded with curcumin, an anticancer drug. The formulation not only improved MRI characteristics and enhanced the anticancer activity of curcumin, but it was also capable of generating localized heat under an AMF, thus showing promise in the treatment of cancer. Matsuoka *et al.* [112] developed magnetite cationic liposomes for treatment of osteosarcoma using localized hyperthermia in hamsters. They achieved the tumor temperature of 42°C, whereas the normal tissues remained unheated. About 12 days after initiation of the study, tumor volume in hamsters treated with SPION hyperthermia was 1/1000-fold smaller than untreated animals.

7. Conclusion

The availability of SPION-based MRI contrast agents refers to the fact that SPIONs may have overcome several biocompatibility and formulation issues and are way ahead of other nanoscale DDSs. Therefore, SPION-based nanoscale DDSs might have the potential for treatment of a diverse range of diseases. The future focus of drug delivery using magnetically driven SPIONs will be on optimizing the synthetic methods

in order to prepare reproducible particles with optimal surface charge, shape, size, biocompatibility and high magnetic moments. Further, researchers should concentrate on improving the specific targeting properties of magnetic DDSs by efficient surface engineering (e.g., determining the optimal frequency, spacing and orientation of functional moieties) and by identification of novel tissue and cellular biomarkers. In addition, more research should be devoted to the stability of SPIONs in colloidal solutions and serum, critical physiological factors that might affect drug delivery outcome (e.g., protein corona) and tuning the balance between protective coating, magnetic moment and other physiochemical properties. These advances should also be coupled with novel strategies, for example, targeting DDSs to endothelial markers in the vicinity of target region or designing NPs which release their cargo in response to the tumor microenvironment. Finally and hopefully, further developments will materialize in the applications of SPIONs in drug delivery across the BBB, intracellular delivery, and for devising multifunctional and theranostic biodevices.

8. Expert opinion

Magnetic NPs usually have a magnetization value in the range of 30 – 50 emu/g [50]. Most clinical magnetic particles or beads are based on ferromagnetic iron oxides with low specific magnetic moments of 20 – 30 emu/g [113]. A higher magnetic moment (> 30 emu/g) may be suitable for SPION's intended use in drug delivery [114,115]. So far, a targeting depth of approximately 10 cm (8 – 12 cm) has been reported in a swine model after intra-arterial infusion of magnetic NPs [116]. The success of SPIONs as DDSs is limited by inadequate magnetic gradients, which stem from the distance between the magnets and the target site. Hypothetically, the magnetic targeting would be more effective in regions closer to the magnets and with slower blood flow. Mathematical simulations have suggested that drug delivery using magnetic systems with an externally applied field seems effective only for targets close to the body surface [117], including, for example, squamous cell carcinoma, malignant melanoma, Kaposi's sarcoma and breast carcinoma. Therefore, superconducting magnets have been used for magnetic drug targeting. Strong external SmBaCuO and YBaCuO bulk superconductors were able to concentrate ferromagnetic particles inside a flow system up to at least 20 mm from the magnet [118] and permanent NdFeB magnets are believed to enhance the depth of magnetic field by up to 10 – 15 cm. Further attempts have been directed to localize the implantation of magnets [119] and application of magnetic stents [120].

Many other issues should be considered while selecting SPIONs for drug delivery, including but not limited to studying the pharmacokinetics and *in vivo* fate of SPIONs, as well as their biodegradability, biocompatibility and potential side effects. More research should be devoted considering the stability of SPIONs in colloidal solutions and in physiological environments [121], critical physiological factors that might affect drug delivery outcome (e.g., protein corona) and tuning the balance between protective coating, magnetic moment and other physiochemical properties. Very recent results revealed that the locally induced temperature around the surface of gold NPs can change the protein corona decoration and alter the biological fate of the NPs [122]. Since SPIONs can be heated up using external magnetic field (more specifically for hyperthermia applications), one should probe their corona variations and biological fate during their hyperthermia applications. The biological interactions of SPION components should also be studied in detail. For instance, in biocompatible silica-coated SPIONs, exposure of the iron oxide core can cause oxidative stress, which may be associated with neurological disorders. Similarly, the degradation products of biocompatible poly(methyl methacrylate) can be toxic.

Surface engineering can have a great impact on future applications of SPIONs. Whereas positively charged PVA-NH_2-coated SPIONs can deliver cargos to the cell nucleus by lysosomal escape, negatively charged PVA-COOH-coated SPIONs show efficacy in attaching themselves to the cell membrane and can be used for targeting the disorders of cell membranes. The discovery of SPION traces in mitochondria created hopes for future applications of SPION-based DDSs to treat mitochondrial disorders and cardiac dysfunctions and even to halt the aging process. Further, as previously shown with other DDSs, SPIONs may be engineered with specific polymers to enhance the potential for crossing the BBB.

Novel SPION-based drug delivery and imaging systems are being developed and transformed rapidly. Li *et al.* [123] fabricated β-cyclodextrin conjugated SPIONs that bind to cholesterol crystals in a selective manner, creating hope for MRI detection of cholesterol crystal-related diseases such as atherosclerosis. In a recent novel work [124], a clinical MRI SPION formulation was used for *ex vivo* photoacoustic nodal staging of melanoma metastases in lymph nodes. In a very recent study [125], pH-responsive SPION micelles were incorporated with β-lapachone which generates ROS stress in cancer cells. The iron ions produced by SPIONs increased the ROS stress generated by β-lapachone by 10-fold and resulted in significantly increased cell death. Another possibility is using drug-free SPIONs for modifying disease; for example, SPIONs have been shown to alter the expression of obesity and type 2 diabetes-associated risk genes in human adipocytes [126]. These examples demonstrate that the applications of SPIONs in molecular therapy are limited only by the imagination and creativity of researchers.

Declaration of interest

The authors have no relevant affiliations or financial involvement with any organization or entity with a financial interest in or financial conflict with the subject matter or materials discussed in the manuscript. This includes employment, consultancies, honoraria, stock ownership or options, expert testimony, grants or patents received or pending or royalties.

Bibliography

1. Kelkar SS, Reineke TM. Theranostics: combining imaging and therapy. Bioconjug Chem 2011;22(10):1879-903
2. Mahmoudi M, Sant S, Wang B, et al. Superparamagnetic iron oxide nanoparticles (SPIONs): development, surface modification and applications in chemotherapy. Adv Drug Deliv Rev 2011;63(1–2):24-46
3. Yen SK, Padmanabhan P, Selvan ST. Multifunctional iron oxide nanoparticles for diagnostics, therapy and macromolecule delivery. Theranostics 2013;3(12):986
4. Anzai Y, Piccoli CW, Outwater EK, et al. Evaluation of neck and body metastases to nodes with ferumoxtran 10–enhanced MR imaging: phase III safety and efficacy study 1. Radiology 2003;228(3):777-88
5. Sakhtianchi R, Minchin RF, Lee K-B, et al. Exocytosis of nanoparticles from cells: role in cellular retention and toxicity. Adv Colloid Interface Sci 2013;201-202:18-29
6. Arruebo M, Galán M, Navascués N, et al. Development of magnetic nanostructured silica-based materials as potential vectors for drug-delivery applications. Chem Mater 2006;18(7):1911-19
7. Durán J, Arias J, Gallardo V, Delgado A. Magnetic colloids as drug vehicles. J Pharm Sci 2008;97(8):2948-83
8. Corot C, Robert P, Idée J-M, Port M. Recent advances in iron oxide nanocrystal technology for medical imaging. Adv Drug Deliv Rev 2006;58(14):1471-504
9. Saei AA, NazhadDolatabadi JE, Najafi-Marandi P, et al. Electrchemical biosensors for glucose based on metal nanoparticles. TrAC Trends Anal Chem 2013;42:216-27
10. Mahmoudi M, Hosseinkhani H, Hosseinkhani M, et al. Magnetic resonance imaging tracking of stem cells in vivo using iron oxide nanoparticles as a tool for the advancement of clinical regenerative medicine. Chem Rev 2010;111(2):253-80
11. Laurent S, Dutz S, Häfeli UO, Mahmoudi M. Magnetic fluid hyperthermia: focus on superparamagnetic iron oxide nanoparticles. Adv Colloid Interface Sci 2011;166(1):8-23
12. Larson TA, Joshi PP, Sokolov K. Preventing protein adsorption and macrophage uptake of gold nanoparticles via a hydrophobic shield. ACS Nano 2012;6(10):9182-90
13. Larsen EKU, Nielsen T, Wittenborn T, et al. Accumulation of magnetic iron oxide nanoparticles coated with variably sized polyethylene glycol in murine tumors. Nanoscale 2012;4(7):2352-61
14. Koffie RM, Farrar CT, Saidi LJ, et al. Nanoparticles enhance brain delivery of blood–brain barrier-impermeable probes for in vivo optical and magnetic resonance imaging. Proc Natl Acad Sci USA 2011;108(46):18837-42
15. Roca A, Costo R, Rebolledo A, et al. Progress in the preparation of magnetic nanoparticles for applications in biomedicine. J Phys D Appl Phys 2009;42(22):224002
16. Lee H, Yu MK, Park S, et al. Thermally cross-linked superparamagnetic iron oxide nanoparticles: synthesis and application as a dual imaging probe for cancer in vivo. J Am Chem Soc 2007;129(42):12739-45
17. Larsen EK, Nielsen T, Wittenborn T, et al. Size-dependent accumulation of PEGylated silane-coated magnetic iron oxide nanoparticles in murine tumors. ACS Nano 2009;3(7):1947-51
18. Zhu XM, Wang YXJ, Leung KCF, et al. Enhanced cellular uptake of aminosilane-coated superparamagnetic iron oxide nanoparticles in mammalian cell lines. Int J Nanomed 2012;7:953
19. Maleki H, Simchi A, Imani M, Costa BFO. Size-controlled synthesis of superparamagnetic iron oxide nanoparticles and their surface coating by gold for biomedical applications. J Magn Magn Mater 2012;324(23):3997-4005
20. Laurent S, Forge D, Port M, et al. Magnetic iron oxide nanoparticles: synthesis, stabilization, vectorization, physicochemical characterizations, and biological applications. Chem Rev 2008;108(6):2064-110
21. Fauconnier N, Pons J, Roger J, Bee A. Thiolation of maghemite nanoparticles by dimercaptosuccinic acid. J Colloid Interface Sci 1997;194(2):427-33
22. Răcuciu M, Creangă D, Airinei A. Citric-acid-coated magnetite nanoparticles for biological applications. Euro Phys J E Soft Matter 2006;21(2):117-21
23. Park J, Lee JJ, Kim IS, et al. Magnetic and MR relaxation properties of avidin–biotin conjugated superparamagnetic nanoparticles. Colloids Surf A 2008;313:288-91
24. Quan Q, Xie J, Gao H, et al. HSA coated iron oxide nanoparticles as drug delivery vehicles for cancer therapy. Mol Pharm 2011;8(5):1669-76
25. Lee YT, Woo K, Choi KS. Preparation of water-dispersible and biocompatible iron oxide nanoparticles for MRI agent. IEEE Trans Nanotechol 2008;7(2):111-14
26. Easo SL, Mohanan PV. Dextran stabilized iron oxide nanoparticles: synthesis, characterization and in vitro studies. Carbohydr Polym 2013;92(1):726-32
27. Rosen JE, Chan L, Shieh DB, Gu FX. Iron oxide nanoparticles for targeted cancer imaging and diagnostics. Nanomedicine 2012;8(3):275-90
28. Lee SJ, Jeong JR, Shin SC, et al. Nanoparticles of magnetic ferric oxides encapsulated with poly (D, L latide-co-glycolide) and their applications to magnetic resonance imaging contrast agent. J Magn Magn Mater 2004;272:2432-3
29. Prashant C, Dipak M, Yang CT, et al. Superparamagnetic iron oxide–Loaded poly (lactic acid)-d-α-tocopherol polyethylene glycol 1000 succinate copolymer nanoparticles as MRI contrast agent. Biomaterials 2010;31(21):5588-97
30. Ai H, Flask C, Weinberg B, et al. Magnetite loaded polymeric micelles as ultrasensitive magnetic resonance probes. Adv Mater 2005;17(16):1949-52
31. Mahmoudi M, Simchi A, Imani M, et al. Optimal design and characterization of superparamagnetic iron oxide nanoparticles coated with polyvinyl alcohol for targeted delivery and imaging. J Phys Chem B 2008;112(46):14470-81
32. Wang Y, Teng X, Wang JS, Yang H. Solvent-free atom transfer radical polymerization in the synthesis of

Fe2O3 polystyrene core-shell nanoparticles. Nano Lett 2003;3(6):789-93

33. Lee HY, Lim NH, Seo JA, et al. Preparation and magnetic resonance imaging effect of polyvinylpyrrolidone coated iron oxide nanoparticles. J Biomed Mater Res B Appl Biomater 2006;79(1):142-50
34. Xu Y-Y, Zhou M, Geng H-J, et al. A simplified method for synthesis of Fe3O4 PAA nanoparticles and its application for the removal of basic dyes. Appl Surf Sci 2012;258(8):3897-902
35. McBain S, Yiu H, El Haj A, Dobson J. Polyethyleneimine functionalized iron oxide nanoparticles as agents for DNA delivery and transfection. J Mater Chem 2007;17(24):2561-5
36. Wu W, He Q, Jiang C. Magnetic iron oxide nanoparticles: synthesis and surface functionalization strategies. Nanoscale Res Lett 2008;3(11):397-415
37. Gomez-Lopera S, Plaza R, Delgado A. Synthesis and characterization of spherical magnetite/biodegradable polymer composite particles. J Colloid Interface Sci 2001;240(1):40-7
38. Schweiger C, Pietzonka C, Heverhagen J, Kissel T. Novel magnetic iron oxide nanoparticles coated with poly (ethylene imine)-g-poly (ethylene glycol) for potential biomedical application: synthesis, stability, cytotoxicity and MR imaging. Int J Pharm 2011;408(1):130-7
39. Al-Deen FN, Selomulya C, Williams T. On designing stable magnetic vectors as carriers for malaria DNA vaccine. Colloids Surf B 2013;102:492-503
40. Tombácz E, Szekeres M, Tóth IY, et al. Colloidal stability of carboxylated iron oxide nanomagnets for biomedical use. Chem Eng 2014;58:3-10
41. Sun X, Ma P, Cao X, et al. Positive hyaluronan/PEI/DNA complexes as a target-specific intracellular delivery to malignant breast cancer. Drug Deliv 2009;16(7):357-62
42. Hofmann-Amtenbrink M, von Rechenberg B, Hofmann H. Superparamagnetic nanoparticles for biomedical applications. Transworld Research Network, Kerala, India, 2009
43. Viali WR, da Silva Nunes E, dos Santos CC, et al. PEGylation of SPIONs by polycondensation reactions: a new strategy to improve colloidal stability in biological media. J Nanoparticle Res 2013;15(8):1-14
44. Huh YM, Jun YW, Song HT, et al. In vivo magnetic resonance detection of cancer by using multifunctional magnetic nanocrystals. J Am Chem Soc 2005;127(35):12387-91
45. Zhang C, Jugold M, Woenne EC, et al. Specific targeting of tumor angiogenesis by RGD-conjugated ultrasmall superparamagnetic iron oxide particles using a clinical 1.5-T magnetic resonance scanner. Cancer Res 2007;67(4):1555-62
46. Bae YH, Park K. Targeted drug delivery to tumors: myths, reality and possibility. J Controlled Release 2011;153(3):198
47. Koo YEL, Reddy GR, Bhojani M, et al. Brain cancer diagnosis and therapy with nanoplatforms. Adv Drug Deliv Rev 2006;58(14):1556-77
48. Longmire M, Choyke PL, Kobayashi H. Clearance properties of nano-sized particles and molecules as imaging agents: considerations and caveats. Nanomedicine 2008;3(5):703-17
49. Choi HS, Liu W, Misra P, et al. Renal clearance of quantum dots. Nat Biotechnol 2007;25(10):1165-70
50. Gupta AK, Gupta M. Synthesis and surface engineering of iron oxide nanoparticles for biomedical applications. Biomaterials 2005;26(18):3995-4021
51. Saito S, Tsugeno M, Koto D, et al. Impact of surface coating and particle size on the uptake of small and ultrasmall superparamagnetic iron oxide nanoparticles by macrophages. Int J Nanomed 2012;7:5415
52. Chouly C, Pouliquen D, Lucet I, et al. Development of superparamagnetic nanoparticles for MRI: effect of particle size, charge and surface nature on biodistribution. J. Microencapsulation 1996;13(3):245-55
53. Osaka T, Nakanishi T, Shanmugam S, et al. Effect of surface charge of magnetite nanoparticles on their internalization into breast cancer and umbilical vein endothelial cells. Colloids Surf B 2009;71(2):325-30
54. Kenzaoui BH, Vilà MR, Miquel JM, et al. Evaluation of uptake and transport of cationic and anionic ultrasmall iron oxide nanoparticles by human colon cells. Int J Nanomed 2012;7:1275
55. Mahmoudi M, Simchi A, Imani M, Haỉfeli UO. Superparamagnetic iron oxide nanoparticles with rigid cross-linked polyethylene glycol fumarate coating for application in imaging and drug delivery. J Phys Chem C 2009;113(19):8124-31
56. Karlsson HL, Cronholm P, Gustafsson J, Moller L. Copper oxide nanoparticles are highly toxic: a comparison between metal oxide nanoparticles and carbon nanotubes. Chem Res Toxicol 2008;21(9):1726-32
57. Ankamwar B, Lai T, Huang J, et al. Biocompatibility of Fe3O4 nanoparticles evaluated by in vitro cytotoxicity assays using normal, glia and breast cancer cells. Nanotechnology 2010;21(7):075102
58. Thoeny HC, Triantafyllou M, Birkhaeuser FD, et al. Combined ultrasmall superparamagnetic particles of iron oxide–enhanced and diffusion-weighted magnetic resonance imaging reliably detect pelvic lymph node metastases in normal-sized nodes of bladder and prostate cancer patients. Eur Urol 2009;55(4):761-9
59. Mahmoudi M, Simchi A, Imani M. Cytotoxicity of uncoated and polyvinyl alcohol coated superparamagnetic iron oxide nanoparticles. J Phys Chem C 2009;113(22):9573-80
60. Mahmoudi M, Simchi A, Vali H, et al. Cytotoxicity and cell cycle effects of bare and poly (vinyl alcohol) coated iron oxide nanoparticles in mouse fibroblasts. Adv Eng Mater 2009;11(12):B243-B50
61. Mahmoudi M, Simchi A, Imani M, et al. A new approach for the in vitro identification of the cytotoxicity of superparamagnetic iron oxide nanoparticles. Colloids Surf B 2010;75(1):300-9
62. Mahmoudi M, Laurent S, Shokrgozar MA, Hosseinkhani M. Toxicity evaluations of superparamagnetic iron oxide nanoparticles: cell "vision" versus physicochemical properties of nanoparticles. ACS Nano 2011;5(9):7263-76
63. Yang WJ, Lee JH, Hong SC, et al. Difference between toxicities of iron oxide magnetic nanoparticles with various surface-functional groups against human normal fibroblasts and fibrosarcoma cells. Materials 2013;6(10):4689-706
64. Jain TK, Reddy MK, Morales MA, et al. Biodistribution, clearance, and biocompatibility of iron oxide magnetic nanoparticles in rats. Mol Pharm 2008;5(2):316-27

65. Weissleder RA, Stark D, Engelstad B, et al. Superparamagnetic iron oxide: pharmacokinetics and toxicity. Am J Roentgenol 1989;152(1):167-73

66. Gaasch JA, Lockman PR, Geldenhuys WJ, et al. Brain iron toxicity: differential responses of astrocytes, neurons, and endothelial cells. Neurochem Res 2007;32(7):1196-208

67. Walczyk D, Bombelli FB, Monopoli MP, et al. What the cell "sees" in bionanoscience. J Am Chem Soc 2010;132(16):5761-8

68. Mahmoudi M, Lohse SE, Murphy CJ, et al. Variation of protein corona composition of gold nanoparticles following plasmonic heating. Nano Lett 2014;14(1):6-12

69. Krol S, Macrez R, Docagne F, et al. Therapeutic benefits from nanoparticles: the potential significance of nanoscience in diseases with compromise to the blood brain barrier. Chem Rev 2013;113(3):1877-903

70. Monopoli MP, Walczyk D, Campbell A, et al. Physical- chemical aspects of protein corona: relevance to in vitro and in vivo biological impacts of nanoparticles. J Am Chem Soc 2011;133(8):2525-34

71. Ghavami M, Saffar S, Emamy BA, et al. Plasma concentration gradient influences the protein corona decoration on nanoparticles. RSC Adv 2013;3(4):1119-26

72. Salvati A, Pitek AS, Monopoli MP, et al. Transferrin-functionalized nanoparticles lose their targeting capabilities when a biomolecule corona adsorbs on the surface. Nat Nanotechnol 2013;8(2):137-43

73. Mirshafiee V, Mahmoudi M, Lou K, et al. Protein corona significantly reduces active targeting yield. Chem Commun 2013;49(25):2557-9

74. Xie J, Xu C, Kohler N, et al. Controlled PEGylation of monodisperse Fe3O4 nanoparticles for reduced non specific uptake by macrophage cells. Adv Mater 2007;19(20):3163-6

75. Ni F, Jiang L, Yang R, et al. Effects of PEG length and iron oxide nanoparticles size on reduced protein adsorption and non-specific uptake by macrophage cells. J Nanosci Nanotechnol 2012;12(3):2094-100

76. Ehrenberg MS, Friedman AE, Finkelstein JN, et al. The influence of protein adsorption on nanoparticle association with cultured endothelial cells. Biomaterials 2009;30(4):603-10

77. Mahmoudi M, Sheibani S, Milani A, et al. Crucial role of protein corona for specific targeting of nanoparticles. Nanomedicine 2014;In press

78. Amiri H, Bordonali L, Lascialfari A, et al. Protein corona affects the relaxivity and MRI contrast efficiency of magnetic nanoparticles. Nanoscale 2013;5(18):8656-65

79. Mahmoudi M, Shokrgozar MA, Sardari S, et al. Irreversible changes in protein conformation due to interaction with superparamagnetic iron oxide nanoparticles. Nanoscale 2011;3(3):1127-38

80. Zhang D, Neumann O, Wang H, et al. Gold nanoparticles can induce the formation of protein-based aggregates at physiological pH. Nano Lett 2009;9(2):666-71

81. Gref R, Lück M, Quellec P, et al. 'Stealth'corona-core nanoparticles surface modified by polyethylene glycol (PEG): influences of the corona (PEG chain length and surface density) and of the core composition on phagocytic uptake and plasma protein adsorption. Colloids Surf B 2000;18(3):301-13

82. Lee H, Lee E, Kim DK, et al. Antibiofouling polymer-coated superparamagnetic iron oxide nanoparticles as potential magnetic resonance contrast agents for in vivo cancer imaging. J Am Chem Soc 2006;128(22):7383-9

83. García KP, Zarschler K, Barbaro L, et al. Zwitterionic-coated "stealth" nanoparticles for biomedical applications: recent advances in countering biomolecular corona formation and uptake by the mononuclear phagocyte system. Small 2014. [Epub ahead of print]

84. Ge C, Du J, Zhao L, et al. Binding of blood proteins to carbon nanotubes reduces cytotoxicity. Proc Natl Acad Sci USA 2011;108(41):16968-73

85. Dominguez-Medina S, Blankenburg J, Olson J, et al. Adsorption of a protein monolayer via hydrophobic interactions prevents nanoparticle aggregation under harsh environmental conditions. ACS Sustain Chem Eng 2013;1(7):833-42

86. Kah JCY, Chen J, Zubieta A, Hamad-Schifferli K. Exploiting the protein corona around gold nanorods for loading and triggered release. ACS Nano 2012;6(8):6730-40

87. Cifuentes-Rius A, de Puig H, Kah JCY, et al. Optimizing the properties of the protein corona surrounding nanoparticles for tuning payload release. ACS Nano 2013;7(11):10066-74

88. Caracciolo G, Cardarelli F, Pozzi D, et al. Selective targeting capability acquired with a protein corona adsorbed on the surface of DOTAP/ DNA nanoparticles. ACS Appl Mater Interfaces 2013;5(24):13171-9

89. Nagayama S, Ogawara KI, Fukuoka Y, et al. Time-dependent changes in opsonin amount associated on nanoparticles alter their hepatic uptake characteristics. Int J Pharm 2007;342(1):215-21

90. Ogawara KI, Furumoto K, Nagayama S, et al. Pre-coating with serum albumin reduces receptor-mediated hepatic disposition of polystyrene nanosphere: implications for rational design of nanoparticles. J Controlled Release 2004;100(3):451-5

91. Kubo T, Sugita T, Shimose S, et al. Targeted delivery of anticancer drugs with intravenously administered magnetic liposomes in osteosarcoma-bearing hamsters. Inter J Oncol 2000;17(2):309-24

92. Widder KJ, Senyei AE, Ranney DF. Magnetically responsive microspheres and other carriers for the biophysical targeting of antitumor agents. Adv Pharmacol Chemother 1979;16:213-71

93. Lübbe AS, Bergemann C, Huhnt W, et al. Preclinical experiences with magnetic drug targeting: tolerance and efficacy. Cancer Res 1996;56(20):4694-701

94. Lübbe AS, Bergemann C, Riess H, et al. Clinical experiences with magnetic drug targeting: a phase I study with 4′-epidoxorubicin in 14 patients with advanced solid tumors. Cancer Res 1996;56(20):4686-93

95. Widder KJ, Morris RM, Poore G, et al. Tumor remission in Yoshida sarcoma-bearing rts by selective targeting of magnetic albumin microspheres containing doxorubicin. Proc Natl Acad Sci USA 1981;78(1):579-81

96. Landfester K, Mailänder V. Nanocapsules with specific targeting and release properties using miniemulsion polymerization. Expert Opin Drug Deliv 2013;10(5):593-609

97. Kong SD, Zhang W, Lee JH, et al. Magnetically vectored nanocapsules for tumor penetration and remotely switchable on-demand drug release. Nano Lett 2010;10(12):5088-92

98. Kong SD, Choi C, Khamwannah J, Jin S. Magnetically vectored delivery of cancer drug using remotely on–off switchable nanocapsules. IEEE Trans Magnet 2013;49(1):349-52

99. Tan H, Wang M, Yang CT, et al. Silica nanocapsules of fluorescent conjugated polymers and superparamagnetic nanocrystals for dual mode cellular imaging. Chem A Eur J 2011;17(24):6696-706

100. Kim TH, Jiang HL, Jere D, et al. Chemical modification of chitosan as a gene carrier in vitro and in vivo. Prog Polym Sci 2007;32(7):726-53

101. Bae KH, Ha YJ, Kim C, et al. Pluronic/chitosan shell cross-linked nanocapsules encapsulating magnetic nanoparticles. J Biomater Sci Polym Ed 2008;19(12):1571-83

102. Kumar A, Jena PK, Behera S, et al. Multifunctional magnetic nanoparticles for targeted delivery. Nanomedicine 2010;6(1):64-9

103. Zhang J, Misra R. Magnetic drug-targeting carrier encapsulated with thermosensitive smart polymer: core–shell nanoparticle carrier and drug release response. Acta Biomater 2007;3(6):838-50

104. Purushotham S, Chang P, Rumpel H, et al. Thermoresponsive core–shell magnetic nanoparticles for combined modalities of cancer therapy. Nanotechnology 2009;20(30):305101

105. Yang X, Grailer JJ, Rowland IJ, et al. Multifunctional stable and pH-responsive polymer vesicles formed by heterofunctional triblock copolymer for targeted anticancer drug delivery and ultrasensitive MR imaging. ACS Nano 2010;4(11):6805-17

106. Yang X, Grailer JJ, Rowland IJ, et al. Multifunctional SPIO/DOX-loaded wormlike polymer vesicles for cancer therapy and MR imaging. Biomaterials 2010;31(34):9065-73

107. Wang CH, Kang ST, Yeh CK. Superparamagnetic iron oxide and drug complex-embedded acoustic droplets for ultrasound targeted theranosis. Biomaterials 2013;34(7):1852-61

108. Ketkar-Atre A, Struys T, Dresselaers T, et al. In vivo hepatocyte MR imaging using lactose functionalized magnetoliposomes. Biomaterials 2014;35(3):1015-24

109. Lamanna G, Kueny-Stotz M, Mamlouk-Chaouachi H, et al. Dendronized iron oxide nanoparticles for multimodal imaging. Biomaterials 2011;32(33):8562-73

110. Walter GA, Cahill KS, Huard J, et al. Noninvasive monitoring of stem cell transfer for muscle disorders. Magn Reson Med 2004;51(2):273-7

111. Yallapu MM, Othman SF, Curtis ET, et al. Multi-functional magnetic nanoparticles for magnetic resonance imaging and cancer therapy. Biomaterials 2011;32(7):1890-905

112. Matsuoka F, Shinkai M, Honda H, et al. Hyperthermia using magnetite cationic liposomes for hamster osteosarcoma. Biomagn Res Technol 2004;2(1):3

113. Qiang Y, Antony J, Sharma A, et al. Iron/iron oxide core-shell nanoclusters for biomedical applications. J Nanopart Res 2006;8(3-4):489-96

114. Hua MY, Yang HW, Liu HL, et al. Superhigh-magnetization nanocarrier as a doxorubicin delivery platform for magnetic targeting therapy. Biomaterials 2011;32(34):8999-9010

115. Rosengart AJ, Kaminski MD. Decorporation of biohazards utilizing nanoscale magnetic carrier systems. Nanofabricat Towards Biomed Appl 2005;343-63

116. Goodwin S, Peterson C, Hoh C, Bittner C. Targeting and retention of magnetic targeted carriers (MTCs) enhancing intra-arterial chemotherapy. J Magn Magn Mater 1999;194(1):132-9

117. Grief AD, Richardson G. Mathematical modelling of magnetically targeted drug delivery. J Magn Magn Mater 2005;293(1):455-63

118. Takeda SI, Mishima F, Fujimoto S, et al. Development of magnetically targeted drug delivery system using superconducting magnet. J Magn Magn Mater 2007;311(1):367-71

119. Forbes ZG, Yellen BB, Halverson DS, et al. Validation of high gradient magnetic field based drug delivery to magnetizable implants under flow. IEEE Trans Biomed Eng 2008;55(2):643-9

120. Chen H, Ebner AD, Kaminski MD, et al. Analysis of magnetic drug carrier particle capture by a magnetizable intravascular stent—2: parametric study with multi-wire two-dimensional model. J Magn Magn Mater 2005;293(1):616-32

121. Mahmoudi M, Meng J, Xue X, et al. Interaction of stable colloidal nanoparticles with cellular membranes. Biotechnol Adv 2013. [Epub ahead of print]

122. Mahmoudi M, Lohse SE, Murphy CJ, et al. Variation of protein corona composition of gold nanoparticles following plasmonic heating. Nano Lett 2014;14(1):6-12

123. Li H, El-Dakdouki MH, Zhu DC, et al. Synthesis of β-cyclodextrin conjugated superparamagnetic iron oxide nanoparticles for selective binding and detection of cholesterol crystals. Chem Commun 2012;48(28):3385-7

124. Grootendorst DJ, Fratila RM, Visscher M, et al. Intra operative ex vivo photoacoustic nodal staging in a rat model using a clinical superparamagnetic iron oxide nanoparticle dispersion. J Biophotonics 2013;6(6-7):493-504

125. Huang G, Chen H, Dong Y, et al. Superparamagnetic iron oxide nanoparticles: amplifying ROS stress to improve anticancer drug efficacy. Theranostics 2013;3(2):116

126. Sharifi S, Daghighi S, Motazacker M, et al. Superparamagnetic iron oxide nanoparticles alter expression of obesity and T2D-associated risk genes in human adipocytes. Sci Rep 2013;3:2173

127. Bhattacharya D, Das M, Mishra D, et al. Folate receptor targeted, carboxymethyl chitosan functionalized iron oxide nanoparticles: a novel ultradispersed nanoconjugates for bimodal imaging. Nanoscale 2011;3(4):1653-62

128. Das M, Mishra D, Maiti T, et al. Bio-functionalization of magnetite nanoparticles using an aminophosphonic acid coupling agent: new, ultradispersed, iron-oxide folate nanoconjugates for cancer-specific targeting. Nanotechnology 2008;19(41):415101

129. Sonvico F, Mornet S, Vasseur S, et al. Folate-conjugated iron oxide nanoparticles for solid tumor targeting as potential specific magnetic hyperthermia mediators: synthesis, physicochemical characterization, and in vitro experiments. Bioconjug Chem 2005;16(5):1181-8

130. Mahajan S, Koul V, Choudhary V, et al. Preparation and in vitro evaluation of folate-receptor-targeted SPION–polymer micelle hybrids for MRI contrast enhancement in cancer imaging. Nanotechnology 2013;24(1):015603

131. Zhang L, Gong F, Zhang F, et al. Targeted therapy for human hepatic carcinoma cells using folate-functionalized polymeric micelles loaded with superparamagnetic iron oxide and sorafenib in vitro. Int J Nanomed 2013;8:1517

132. Kaaki K, HervèI -Aubert K, Chiper M, et al. Magnetic nanocarriers of doxorubicin coated with poly (ethylene glycol) and folic acid: relation between coating structure, surface properties, colloidal stability, and cancer cell targeting. Langmuir 2011;28(2):1496-505

133. Maeng JH, Lee DH, Jung KH, et al. Multifunctional doxorubicin loaded superparamagnetic iron oxide nanoparticles for chemotherapy and magnetic resonance imaging in liver cancer. Biomaterials 2010;31(18):4995-5006

134. Guo M, Que C, Wang C, et al. Multifunctional superparamagnetic nanocarriers with folate-mediated and pH-responsive targeting properties for anticancer drug delivery. Biomaterials 2011;32(1):185-94

135. Lin JJ, Chen JS, Huang SJ, et al. Folic acid–Pluronic F127 magnetic nanoparticle clusters for combined targeting, diagnosis, and therapy applications. Biomaterials 2009;30(28):5114-24

136. Kohler N, Sun C, Wang J, Zhang M. Methotrexate-modified superparamagnetic nanoparticles and their intracellular uptake into human cancer cells. Langmuir 2005;21(19):8858-64

137. Kohler N, Sun C, Fichtenholtz A, et al. Methotrexate immobilized poly (ethylene glycol) magnetic nanoparticles for MR imaging and drug delivery. Small 2006;2(6):785-92

138. Taratula O, Garbuzenko O, Savla R, et al. Multifunctional nanomedicine platform for cancer specific delivery of siRNA by superparamagnetic iron oxide nanoparticles-dendrimer complexes. Curr Drug Deliv 2011;8(1):59-69

139. Leuschner C, Kumar CS, Hansel W, Hormes J. Targeting breast cancer cells and their metastases through luteinizing hormone releasing hormone (LHRH) receptors using magnetic nanoparticles. J Biomed Nanotechol 2005;1(2):229-33

140. Kim DK, Chang JH, Kang YJ. Efficient internalization of peptide-conjugated SPIONs in dendritic cells for tumor targeting. J Nanosci Nanotechnol 2012;12(7):5191-8

141. Cho H-S, Dong Z, Pauletti GM, et al. Fluorescent, superparamagnetic nanospheres for drug storage, targeting, and imaging: a multifunctional nanocarrier system for cancer diagnosis and treatment. ACS Nano 2010;4(9):5398-404

142. El-Dakdouki MH, Zhu DC, El-Boubbou K, et al. Development of multifunctional hyaluronan-coated nanoparticles for imaging and drug delivery to cancer cells. Biomacromolecules 2012;13(4):1144-51

143. Yu MK, Park J, Jeong YY, et al. Integrin-targeting thermally cross-linked superparamagnetic iron oxide nanoparticles for combined cancer imaging and drug delivery. Nanotechnology 2010;21(41):415102

144. Wu C, Gong F, Pang P, et al. An RGD-modified MRI-visible polymeric vector for targeted siRNA delivery to hepatocellular carcinoma in nude mice. PLoS One 2013;8(6):e66416

145. Yang X, Hong H, Grailer JJ, et al. cRGD-functionalized, DOX-conjugated, and 64Cu-labeled superparamagnetic iron oxide nanoparticles for targeted anticancer drug delivery and PET/MR imaging. Biomaterials 2011;32(17):4151-60

146. Cavalli S, Carbajo D, Acosta M, et al. Efficient gamma-amino-proline-derived cell penetrating peptide–superparamagnetic iron oxide nanoparticle conjugates via aniline-catalyzed oxime chemistry as bimodal imaging nanoagents. Chem Commun 2012;48(43):5322-4

147. Sun C, Fang C, Stephen Z, et al. Tumor-targeted drug delivery and MRI contrast enhancement by chlorotoxin-conjugated iron oxide nanoparticles. Nanomedicine (Lond) 2008;3(4):495-505

148. Veiseh O, Gunn JW, Kievit FM, et al. Inhibition of tumor cell invasion with chlorotoxin bound superparamagnetic nanoparticles. Small 2009;5(2):256-64

149. Veiseh O, Kievit FM, Fang C, et al. Chlorotoxin bound magnetic nanovector tailored for cancer cell targeting, imaging, and siRNA delivery. Biomaterials 2010;31(31):8032-42

150. Kievit FM, Veiseh O, Fang C, et al. Chlorotoxin labeled magnetic nanovectors for targeted gene delivery to glioma. ACS Nano 2010;4(8):4587-94

151. Kumar M, Yigit M, Dai G, et al. Image-guided breast tumor therapy using a small interfering RNA nanodrug. Cancer Res 2010;70(19):7553-61

152. Yu MK, Kim D, Lee IH, et al. Image guided prostate cancer therapy using aptamer functionalized thermally cross linked superparamagnetic iron oxide nanoparticles. Small 2011;7(15):2241-9

153. Wang AZ, Bagalkot V, Vasilliou CC, et al. Superparamagnetic iron oxide nanoparticle–aptamer bioconjugates for combined prostate cancer imaging and therapy. ChemMedChem 2008;3(9):1311-15

154. Min K, Jo H, Song K, et al. Dual-aptamer-based delivery vehicle of doxorubicin to both PSMA (+) and PSMA (-) prostate cancers. Biomaterials 2011;32(8):2124-32

155. Chen W, Cao Y, Liu M, et al. Rotavirus capsid surface protein VP4-coated Fe3O4 nanoparticles as a theranostic platform for cellular imaging and drug delivery. Biomaterials 2012;33(31):7895-902

156. Chen G, Chen W, Wu Z, et al. MRI-visible polymeric vector bearing CD3 single chain antibody for gene delivery to T cells for immunosuppression. Biomaterials 2009;30(10):1962-70

157. Yang C, Rait A, Pirollo KF, et al. Nanoimmunoliposome delivery of superparamagnetic iron oxide markedly enhances targeting and uptake in human cancer cells in vitro and in vivo. Nanomedicine 2008;4(4):318-29

158. Jiang W, Xie H, Ghoorah D, et al. Conjugation of functionalized SPIONs

with transferrin for targeting and imaging brain glial tumors in rat model. PLoS One 2012;7(5):e37376

159. Liang S, Wang Y, Yu J, et al. Surface modified superparamagnetic iron oxide nanoparticles: as a new carrier for bio-magnetically targeted therapy. J Mater Sci Mater Med 2007;18(12):2297-302

160. Zou P, Yu Y, Wang YA, et al. Superparamagnetic iron oxide nanotheranostics for targeted cancer cell imaging and pH-dependent intracellular drug release. Mol Pharm 2010;7(6):1974-84

161. Kievit FM, Stephen ZR, Veiseh O, et al. Targeting of primary breast cancers and metastases in a transgenic mouse model using rationally designed multifunctional SPIONs. ACS Nano 2012;6(3):2591-601

162. Hadjipanayis CG, Machaidze R, Kaluzova M, et al. EGFRvIII antibody–conjugated iron oxide nanoparticles for magnetic resonance imaging–guided convection-enhanced delivery and targeted therapy of glioblastoma. Cancer Res 2010;70(15):6303-12

Affiliation

Sophie Laurent[†1], Amir Ata Saei[2,3], Shahed Behzadi[4], Arash Panahifar[5] & Morteza Mahmoudi[*3,6]

[†,*]Authors for correspondence

[1]University of Mons, Avenue Maistriau, NMR and Molecular Imaging Laboratory, Department of General, Organic, and Biomedical Chemistry, 19, B-7000 Mons, Belgium
E-mail: sophie.laurent@umons.ac.be

[2]Tabriz University of Medical Sciences, School of Pharmacy, Research Center for Pharmaceutical Nanotechnology, Tabriz, Iran

[3]Tehran University of Medical Sciences, Nanotechnology Research Center, Department of Nanotechnology, Faculty of Pharmacy, Tehran, Iran
E-mail: Mahmoudi@stanford.edu

[4]Max Planck Institute for Polymer Research, Ackermannweg 10, 55128 Mainz, Germany

[5]University of Alberta, Faculty of Pharmacy and Pharmaceutical Sciences, Edmonton, Alberta, Canada

[6]Stanford University, School of Medicine, Division of Cardiology, Department of Pediatrics, Stanford, CA, USA